OULUN YLIOPISTO
UNIVERSITY of OULU

FACULTY OF TECHNOLOGY

The measurement and modeling of snowmelt in sub-arctic site using low cost temperature loggers

Leo-Juhani Meriö

Master's Thesis
Environmental Engineering
July 2015

ABSTRACT
FOR THESIS

University of Oulu Faculty of Technology

Degree Programme	**Major Subject**
Environmental Engineering	Water and Geoenvironmental Engineering
Author	**Thesis Supervisor**
Meriö, Leo-Juhani	D.Sc. Marttila H., D.Sc. Ala-aho P. and prof. Kløve B.

Title of Thesis

The measurement and modeling of snowmelt in sub-arctic site using low cost temperature loggers

Major Subject	**Type of Thesis**	**Submission Date**	**Number of Pages**
Water and Geoenvironmental Engineering	Master's Thesis	July 2015	79, 2 annexes

Abstract

The aim of this thesis was to study and test how inexpensive temperature loggers can be used to measure the local and microscale variability of the snowmelt processes and rates in subarctic Pallastunturi fell area.

The loggers were deployed on six test plots with varied topography, vegetation and terrain type. In each test plot the sensors were installed in five test points on the ground and above the ground on fixed height of 30 cm. During the installation, the snowpack height and density were measured from each test point. The temperature was recorded at 15 min interval from 19th of April to 15th of June 2014. The melting processes and rates were determined using diurnal temperature fluctuations of the sensors. Validity of the results was evaluated using snow height data from adjacent measurement stations maintained by Geological Survey of Finland, equipped with acoustic snow sensor. Additionally an empirical snow model was employed to test the determined melt rates using climate data from Finnish Meteorological Institute as input for the model.

The results exposed the difference in timing and variability of the snowmelt. Timing was earlier in southern slopes and slightly earlier in open areas compared forests. The variability of the melt timing was highest at forested plots whereas it was lowest at an open mire. The results agreed reasonably well with the measurement results from the acoustic measurement station but gave also information about the spatial variability of the melt.

Determined melt rates were used in an empirical degree-day snow model to estimate the snow water equivalent between 1st of September 2013 to 31st of August 2014. The root mean squared error between the model and measured dates for the end of permanent snow cover for the data from 24 test points was 3.74 days. The microscale accuracy of the method was highest in relatively homogenous and open terrain type, such as open mire, where the accuracy was approximately one day. In more complex terrain types with forests the method was less accurate, thus median determined melt rates are recommended to be used in such conditions.

Solar radiation absorbed by the logger resulting to increased melt speed near the sensor was assessed to be among the most significant sources of uncertainty for the method. Other significant factors resulting to inaccuracy in melt rate determination include possible dislocation of the upper sensor due to snow compression during the spring and unknown physical properties of the snow during the final melt period.

Despite the uncertainties, regions where the current snow measurements are not representative and remote ungauged catchments are assessed to be especially suitable for using the method presented in this study. Loggers equipped with wireless connections could be additionally used for real-time tracking of the snow accumulation and melt.

Additional Information

TIIVISTELMÄ
OPINNÄYTETYÖSTÄ Oulun yliopisto Teknillinen tiedekunta

Koulutusohjelma Ympäristötekniikka	**Pääaineopintojen ala** Vesi- ja geoympäristötekniikka
Tekijä Meriö, Leo-Juhani	**Työn ohjaaja yliopistolla** TkT Marttila H., TkT Ala-aho P. ja prof. Kløve B.

Työn nimi
Lumen sulannan mittaus ja mallintaminen subarktisella alueella edullisten lämpötilatallentimien avulla

Opintosuunta	**Työn laji**	**Aika**	**Sivumäärä**
Vesi – ja geoympäristötekniikka	Diplomityö	Heinäkuu 2015	79, 2 liitettä

Tiivistelmä

Työn tavoitteena oli selvittää ja testata miten edullisia lämpötilatallentimia voidaan käyttää lumen sulannan prosessien ja nopeuden mittaamiseen subarktisella Pallaksen tunturialueella.

Lämpötila-anturit sijoitettiin kuudelle koealueelle, joiden topografia, kasvillisuus ja maastotyyppi vaihtelevat. Tallentimet asennettiin jokaisella koealueella viiteen koepisteeseen sekä maahan että 30 cm vakiokorkeudelle maanpinnasta. Asennuksen aikana mitattiin lumipeitteen korkeus ja tiheys jokaiselta koepisteeltä. Anturit ohjelmoitiin tallentamaan lämpötila 15 min välein 19.4. – 15.6.2014 välisenä aikana. Lumen sulannan nopeus määritettiin antureiden päivittäisen lämpötilavaihtelun avulla. Tulosten oikeellisuutta arvioitiin vertaamalla niitä koealueella sijaitsevien Geologian tutkimuskeskuksen akustisien sensorien mittaamiin lumenkorkeustietoihin. Lisäksi määritettyjä lumen sulannan nopeutta kuvaavia astepäivätekijöitä testattiin empiirisellä lumimallilla, jonka lähtötietoina käytettiin Ilmatieteen laitoksen ilmastoaineistoa.

Tulokset paljastivat lumen sulannan ajankohdan sekä sen vaihtelun. Sulaminen tapahtui aikaisemmin eteläisillä rinteillä verrattuna pohjoisiin sekä hieman aikaisemmin avoimilla alueilla kuin metsässä. Sulamisajankohdan vaihtelu oli suurinta metsäalueilla ja pienintä avoimella suolla. Tulokset vastasivat kohtuullisen hyvin akustisella lumenkorkeussensorilla mitattuja arvoja, mutta lisäksi saatiin tietoa sulannan alueellisesta vaihtelusta.

Mittaustulosten avulla määritettyjä sulamisnopeuksia ja empiiristä astepäivätekijämallia hyödyntäen mallinnettiin lumen vesiarvo jokaisessa koepisteessä välillä 1.9.2013 – 31.8.2014. Keskineliövirheen neliöjuuri (RMSE) mallinnetun ja mitatun pysyvän lumipeitteen lähtemispäivämäärän välillä oli 3.74 päivää. Paras tarkkuus (noin yksi päivä) saavutettiin suhteellisen homogeenisellä ja avonaisella alueella, avoimella suolla. Topografian ollessa vaihtelevampaa sekä metsäisillä alueilla menetelmän tarkkuus heikkeni, mutta käyttämällä koealuekohtaista sulamisnopeuden mediaania tarkkuutta saatiin parannettua.

Merkittävimpiä menetelmän epävarmuustekijöitä arvioitiin olevan auringonsäteily, joka lämmittää lämpötilatallenninta ja sulattaa lumen nopeammin tallentimen läheisyydestä. Lisäksi osassa koepisteitä havaittu ylempien tallentimien lumen painumisen aiheuttama siirtyminen alaspäin sekä sulannan loppuvaiheessa tuntemattomat lumen fysikaaliset ominaisuudet voivat aiheuttaa merkittävää virhettä sulamisnopeuden arvioimisessa.

Epävarmuustekijöistä huolimatta menetelmän arvioidaan sopivan erityisesti alueille, joilla tämän hetkiset lumimittaukset eivät ole edustavia, sekä etäisille valuma-alueille, joita ei aikaisemmin ole mitattu. Langattomalla yhteydellä varustettuja lämpötilatallentimia voitaisiin lisäksi käyttää reaaliaikaiseen lumen kertymisen ja sulamisen seurantaan.

Muita tietoja

FOREWORD / AKNOWLEDGEMENTS

The purpose of this master's thesis was to study the snow melt processes and test how inexpensive temperature loggers could be used to measure the snow melt processes and rates in subarctic region. The study was done mainly between December 2014 and June 2015 in Water Resources and Environmental Engineering Research Group, University of Oulu, which also provided funding for the work.

I would like to thank my supervisor Bjørn Kløve for the guidance and valuable comments for the work. Further thanks goes to my supervisors Hannu Marttila and Pertti Ala-aho for the advice for the working methods, improvement ideas for the structure, contents and figures of the thesis and especially for the much appreciated encouragement throughout the process.

This thesis would not have been possible without field work. Extra thanks goes to Pertti Ala-aho and his team for deploying the loggers and doing the snow pack measurements on spring 2014. Thanks to Romain Boche and Elodie Jacquel for the help in field work on summer 2014.

I also want to thank the people at Geological Survey of Finland, Finnish Environment Institute and Finnish Meteorological Institute for the material and comments for this thesis. Thanks also to Veikko Pekkala, Pauliina Björk, Anna Jaros, Tuomo Reinikka and all the others who gave advice and comments for the work.

Finally, family and friends, my deepest gratitude goes to you for the understanding and support even during the numerous evenings and weekends I spent with the studies neglecting my other duties and privilegies.

Oulu, 25th of June 2015

Leo-Juhani Meriö

CONTENTS

ANNEXES:

ABBREVIATIONS AND SYMBOLS

CC	Cold content
CCD	Cloud condensing nuclei
CCF	Cold-content degree-day factor
CF_r	Correction factor for liquid precipitation
CF_s	Correction factor for snow precipitation
CV	Coefficient of Variation
DDF	Degree-Day Factor
E	Evaporation
FMI	Finnish Meteorological Institute
FSC	Fractional Snow Cover
f	Maximum liquid water content in the snowpack
GTK	Geological Survey of Finland
h_m	Snow water equivalent
h_s	Height of the snowpack
IPPC	Intergovernmental Panel on Climate Change
IQR	Interquartile Range
LWR	Long Wave Radiation
LWHC	Liquid Water Holding Capacity
LWRC	Liquid Water Retention Capacity
M	Amount of snowmelt
masl	meters above sea level
NASA	National Aeronautics and Space Administration
O	Outflow
P_r	Liquid precipitation
P_s	Snow precipitation
R^2	Coefficient of determination
RMSE	Root mean square error
SCA	Snow Covered Area
SD	Standard Deviation
SYKE	Finnish Environment Institute
SWE	Snow Water Equivalent
SWR	Short Wave Radiation

TSF	Surface Temperature Factor
T_a	Air temperature
T_{crit}	Critical temperature for snow precipitation
T_m	Melting temperature of snow
T_s	Surface temperature of the snowpack
δ_s	Density of snow
δ_w	Density of water
WHC	Water Holding Capacity

1 INTRODUCTION

Snow has a substantial impact on the environment at the high latitudes where the permanent snow cover can last for 200 – 220 days (Vajda et al. 2006) and over 40 % of the annual precipitation can fall as snow (Sutinen et al. 2012; Jones 2001). The snow accumulated during winter acts as a water storage which is drained during the snow melt period in spring. The melt of the snowpack has a significant impact on the hydrology in high latitudes being usually the largest individual event during the hydrologic year, manifested as high ground water levels, peak annual flows in the rivers and occasional floods (Okkonen and Kløve 2011).

According to Rasmus (2005) the snow distribution and processes have a high variability depending on the catchment and climate conditions. Information of timing and rates of the snowmelt is needed to predict the magnitude and timing of the floods, to control the flow in regulated rivers for dam safety and to ensure adequate environmental flow. The measurements of the snowpack properties are usually discontinuous and the network is often very sparse due to high resource needs. Thus, there is a demand for quick and inexpensive method for snowmelt measurements. Additionally such method could be used as first tool in research of previously unexplored areas.

The aim of this thesis is to test and study how low cost temperature loggers can be used to measure local and microscale variability of the snowmelt processes and rates at subarctic Pallastunturi fell area. Field techniques, statistical analysis and an empirical snow model are used as tools for the study.

Loggers were installed on six locations with different topography, vegetation and terrain type to record snowpack temperatures. Topical snowpack properties were measured during the installation. Fluctuations of the logger temperatures were used to determine the melting processes and rates. Adjacent stationary measurement station equipped with acoustic snow measurement sensor was used to validate the results. The impact of measured snow properties, vegetation and topography to snow melt was studied with correlation analysis.

The accumulation and melt of the snowpack were estimated with an empirical snow model incorporating estimates for spatial and temporal development of snow water

equivalent, cold content and liquid water content of the snowpack during period from 1st of September 2013 to 31st of August 2014. Climate data from adjacent measurement site was used as the input for the model. The modelled snowpack was compared with the measurement results and validity of the model was evaluated.

2 THEORY

2.1 Snowmelt in the hydrologic cycle

Water on the planet earth is in continuous natural movement and change between solid, liquid and vapor phases. The driving forces are the energy from the sun and the gravity of the earth (Dingman 2008, p. 48). This water movement on the surface, soil and atmosphere of the earth forms the global water cycle (Figure 1), i.e. the hydrological cycle.

Oceans are the major contributors to the global hydrologic cycle by receiving 79 % of the precipitation and producing 88 % of the evapotranspiration. Thus, the land surface of the earth receives more water as precipitation than which is lost due to evapotranspiration. The excess water is available for the land phase of the hydrologic cycle until it is finally discharged back to the oceans. (Dingman 2008, p. 49)

The land phase of the hydrologic cycle at high latitudes is affected by annual snow cover. A substantial part of the precipitation is falling as snow creating a clear seasonal cycle in the area. The snow accumulates on winter and acts as a storage for the water. During spring the snowpack melts producing surface runoff and groundwater recharge. The impact of the snow melt can be seen as the maximum annual discharge and floods in the rivers and river plains as well as increased groundwater levels in the soil (Okkonen and Kløve 2011). The meltwater from the snow acts usually as the main input to the hydrology in the sub-arctic areas. (Dingman 2008, p. 166; Veijalainen 2012, p. 22)

The Intergovernmental Panel on Climate Change (IPPC 2013b) presented research results in Assessment Report 5 (AR5), which indicate that the global surface temperature has warmed substantially in the past and the warming will continue. The temperature is predicted to increase at the end of 21st century as much as 4.8°C in the worst case scenario (Regional Concentration Pathway, RCP8.5 which increases the radiative forcing by 8.5 W m^{-2}). Warming will be faster than the mean in Arctic region and higher on continents than sea (with very high confidence). (IPPC 2013a)

The increased surface temperatures can lead to reduction of the global snow covered area which has a negative impact on the global energy budget accelerating global warming as

the snow cover reflects a large part of the irradiance back to the atmosphere, reducing the heating of the earth surface (Jones 2001). Warming climate will potentially shift the spring flood peaks earlier to winter, decreasing the availability of water during summer, when the need is highest (Barnett et al. 2005). Thus, it is important to study the properties of the snow and develop new measurement methods.

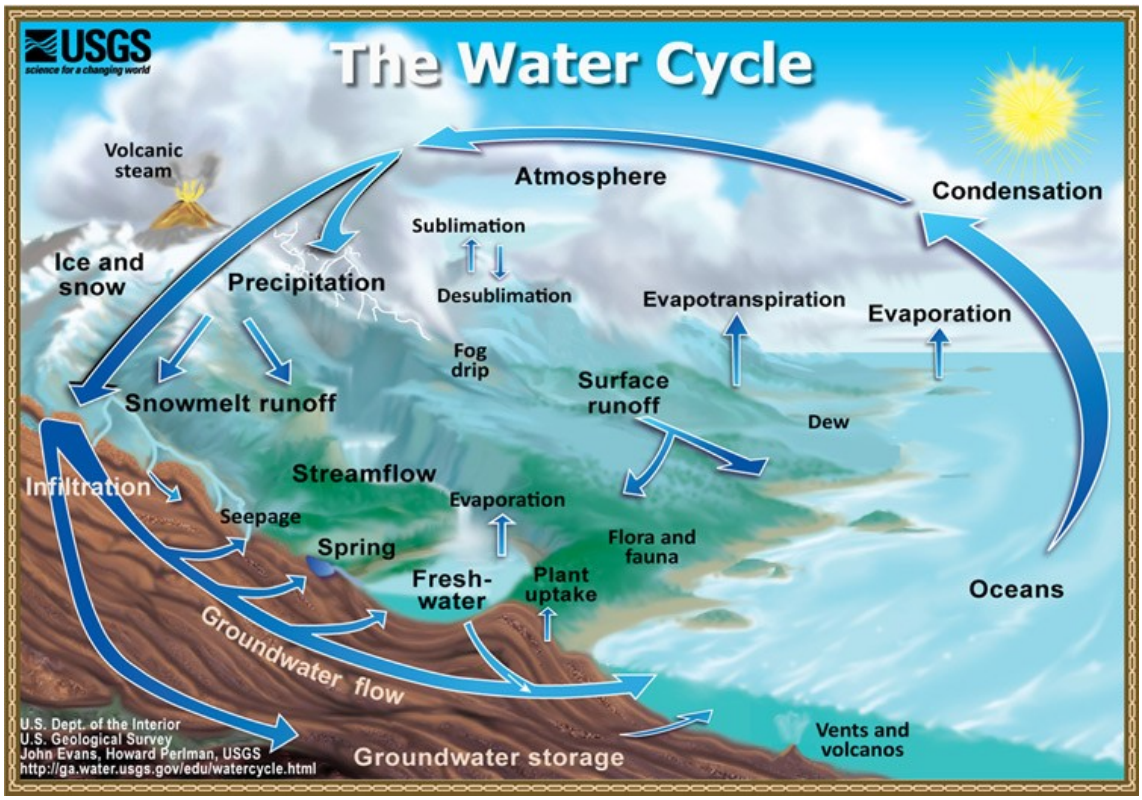

Figure 1. The hydrologic cycle. (Picture: USGS 2015)

2.2 Properties of snow

Snow can be described as a porous medium consisting of ice and pore spaces. When the temperature is below the melting point of ice, the snow is a two phase system with pores filled with air including water vapor. This kind of snow is defined as dry. After the temperature is at the melting point of water or above the snow is considered wet, a three phase system with pores containing also liquid water. (Dingman 2008, p. 166)

The amount of liquid water in the snowpack is called liquid water content. In addition to temperature, it depends on the rate of melt in the snowpack, rainfall on the snow surface, liquid water retention capacity of snow and the rate of water draining from the snowpack (Jones 2001). According to Kuusisto (1986, p. 53) the liquid water retention capacity decreases during the snowmelt because of increasing grain size of snow. Other

explanation include the formation of preferential melt water pathways (Kuusisto 1984, p. 71; Pomeroy and Brun 2001, p. 46).

As the snow is actually a reservoir of water, in form of solid ice and liquid water, it's important to know the amount of total water it contains, i.e. the snow water equivalent (SWE). It can be calculated when the density and height of the snowpack are known in a defined pillar of snow (Dingman 2008). SWE is usually expressed as height and can be calculated with equation

$$h_m = h_s \times \frac{\delta_s}{\delta_w} \quad (1)$$

where h_m is the snow water equivalent (m)
h_s is the height of the snowpack (m)
δ_s is the density of the snow (kg m^{-3})
δ_w is the density of the water (kg m^{-3}).

The thermal conductivity of the snow is relatively low and is a function of the density and the liquid water content of the snowpack. The thermal conductivity starts to increase with the square of density, when the density reaches 200 kg m^{-3}. Because of this non-linear behavior the insulation properties of non-homogenous snowpack are higher than a homogenous snowpack of same height and density. Density of the snowpack typically increases during the snow season due to metamorphosis (Chapter 2.3.2) which leads also to increase in thermal conductivity. Typical value for dry snow with density of 100 kg m^{-3} is 0.045 W m^{-1} K^{-1}. Other important thermal properties of snow are the latent heat of vaporization, which is extremely large, approximately 2.83 MJ kg^{-1} and latent heat of fusion, i.e. melt, which is also large, approximately 333 kJ kg^{-1}. Heat capacity of ice is approximately 2.102 kJ kg^{-1} K^{-1}. (Dingman 2008)

Albedo describes the ratio of incoming shortwave radiation to the reflected shortwave radiation, which has a substantial effect to the energy balance of melting snow. The albedo is highest for fresh snow (90 %) and decreases until the end of melt season (20 %) (Kuusisto 1984; Rasmus 2005). Because of the porous nature of the snow, the shortwave radiation is reflected also below the surface of the snowpack. The shortwave radiation penetrates 20 - 30 cm below the snow surface (Pomeroy and Brun 2001). According to

(Gray 1981) the albedo starts to decrease at snow depths below 12 cm as the radiation starts to be absorbed by the underlying ground. In conifer forest the albedo of the intercepted snow is found to be substantially lower than the snow on the ground snowpack, resulting faster melting and higher evaporation for the snow intercepted by the canopy (Dingman 2008, p. 195).

2.3 Snow accumulation

Precipitation of solid ice crystals, i.e. snow flakes, graupel and hail can be defined as snowfall. The formation of ice crystals aloft in the troposphere is a complex process which is depending of the degree of water saturation in the clouds, temperature and the availability of cloud condensing nuclei, CCD (Dingman 2008, p. 592). Wallace and Hobbs (1977) cited by Pomeroy and Brun (2001) found that the air from marine environment contains more CCD than air from continental environment, which makes the precipitation more likely from the former. If the temperature rises above 0 °C during the snow crystal is falling to ground it can melt partially or completely. The ratio between ice and water is depending of the altitude of the 0 °C front in the atmosphere (Dingman 2008, p. 103).

The conditions of the atmosphere as a function of altitude are not normally known. Thus simplified approaches are developed to estimate the ratio between liquid and solid precipitation. Air temperature is found to be a good predictor for the fractions by Hankimo (1976) according to Kuusisto (1984, p. 28). Uncertainties in estimating precipitation type using air temperature in conditions with long and cold winters are found especially at the beginning and end of the period of permanent snow cover (Vehviläinen 1992).

The density of freshly fallen snow depends mainly on the air temperature, humidity and wind. Relative humidity during snowfall was found to be the most important predictor for snow density by Meløysund et al. (2007), which in a way incorporates the effect of temperature. Generally the density is increasing when the air temperature is rising and the wind is increasing. The density range of new snow has been found to be from 60 kg m^{-3}, in cold and calm, to 340 kg m^{-3} in windy and high temperature conditions. For practical reasons, mainly due to difficulties in measurements, the density is often assumed to be 100 kg m^{-3} for freshly fallen snow. (USACE 1956; Dingman 2008)

2.3.1 Distribution

Accumulated snow can have big spatial variability even in a small area depending on meteorological conditions, topography and vegetation. The varied factors include depth and density, thus also the snow water equivalent. The meteorological conditions affect to the initial formation of the snowpack. Wind transports the snow after the deposition, depending on the properties of the snow and the environment. Typically dry snow with lower density in open areas is more affected. The impact of wind include erosion of snow cover caused by the shear force, transport of the snow from exposed locations where the aerodynamic surface roughness is low, sublimation of snow during the transport and deposition of snow to areas where the aerodynamic roughness is higher or the exposure to wind is lower (Pomeroy and Brun 2001). Topography and vegetation impact the meteorological factors by e.g. affecting the temperature and wind conditions but they can also have direct effect by e.g. interception of the snow by canopy cover (Dingman 2008, p. 195). According to Pomeroy and Brun (2001), the depth of the snow cover is increasing with the elevation if vegetation and micro-relief are invariable. The increase is higher where the wind is ascending the mountain. However, in studies at western Canadian mountains show that change is rather small below 600 masl. In northern Finland fell area (Lommoltunturi) the thickness of the snowpack is found to be lower in tree line and open tundra than in forest area on lower elevations (Sutinen et al. 2012).

The variability of snow is divided into three different scales defined by Kuusisto (1984, p. 30): microscale, mesoscale and macroscale variability. Regional, local and microscale naming is used e.g. by Rasmus (2005).

- Microscale variability is defined to be the variability of snow in a homogenous area with range from few centimeters to 100 m. The characteristics of the area can be an open field in a forest, area of a uniform forest or any terrain type of constant aspect and slope.
- Mesoscale (local) variability is a result of variation of topographic factors and vegetation, such as the type of terrain, aspect, slope or density of the forest. The range varies typically from few tens of meters to kilometers.
- Macroscale (regional) variability is the variation resulted by the climatologic factors. Typically the range is from a few kilometers near coast to several hundred kilometers.

2.3.2 Metamorphosis

Immediately after the snow reaches the ground it begins to change its form. This process is called the metamorphosis of the snow. During the process the structure of snow transforms from crystals to granules (Brass 1990, p. 256). Dingman (2008, p. 167-168) divides the metamorphosis into four mechanisms which are: gravitational settling, destructive metamorphosis, constructive metamorphosis and melt metamorphosis.

The gravitational settling is caused by the weight of the overlying snow layer and is increased with the temperature and decreased with the density of the layer. The rates of increasing density can be between 2 to 50 kg m^{-3} d^{-1}. (Anderson 1973 according to Dingman 2008, p. 168)

The destructive metamorphosis depends on the curvature of the snowflakes. The smaller convex surfaces of the snowflakes are evaporating and freezing again to the less convex surfaces. According to Dingman (2008) this happens due to higher vapor pressures in the areas where the radius of the convex surface of the snowflake is smaller. The effect is fastest for freshly fallen snow, increase of density about 1 % h^{-1} and leads to more spherical shaped grains of snow. (Dingman 2008)

The most important process before the melt season is constructive metamorphosis. It happens over short distances by sintering process, where snow grains are merged together by water molecules deposited between them. Over longer distances the constructive metamorphosis can happen because of temperature gradients in the snowpack. The water is sublimated in the warmer areas and the vapor is transported to the colder areas, due to temperature gradient, where it condensates. Especially when the air temperature is very cold the temperature gradient in the snowpack can be very high, which causes the snowpack to evaporate near the ground in relatively high rates. In these conditions a low density and strength basal layer, called depth hoar, is formed close to the ground. (Dingman 2008)

Finally the melt metamorphosis can be divided to two processes. Firstly, latent heat warming the snowpack is released when the melt snow or rain precipitation falling on the snowpack freezes again. Secondly, liquid water in the snowpack results in rapid loss of smaller snow grains and formation of larger. Due to this process the actively melting snowpack consists of rounded grains with size from 1 to 3 mm (Dingman 2008, p. 204).

The result of the described metamorphosis processes is that the density is increasing progressively during the snow accumulation season, except during the new snowfall and formation of depth hoar (Dingman 2008). Kuusisto (1986) found that the increase in snowpack density is high during the first half of the melt season but the increase halts during the second half because of the increased grain size, thus decreasing the liquid water holding capacity.

2.4 Snowmelt

2.4.1 Energy budget of the snowpack

The snowmelt processes are controlled by the mass and energy exchange between snow cover and the environment (Figure 2). According to DeWalle and Rango (2011, p. 146) the primary contribution occurs at the interface between the snowpack and atmosphere. The energy is transferred mainly by short and longwave radiation, convective and turbulent transfer of sensible heat by difference between temperature of the air and snow and latent heat by vapor exchange. Smaller amounts of energy are added by the warm rainfall and heat conduction from the ground.

Conceptually, the physical snowmelt begins after the net energy input exceeds the cold content of the snowpack. The cold content equals to the energy needed to warm the snowpack to the isothermal 0 °C, i.e. to the melting point of ice. The excess energy is available for snowmelt. In natural environment the melting can start already from the surface even if the temperature lower in the snowpack is still below melting point. According to Pomeroy and Brun (2001) the rate of snowmelt is controlled by the energy balance of the near surface layer. Because of the low heat conductivity of snow, the melting can occur near the base of the snowpack even the air temperature is significantly below 0 °C (Kuusisto 1984).

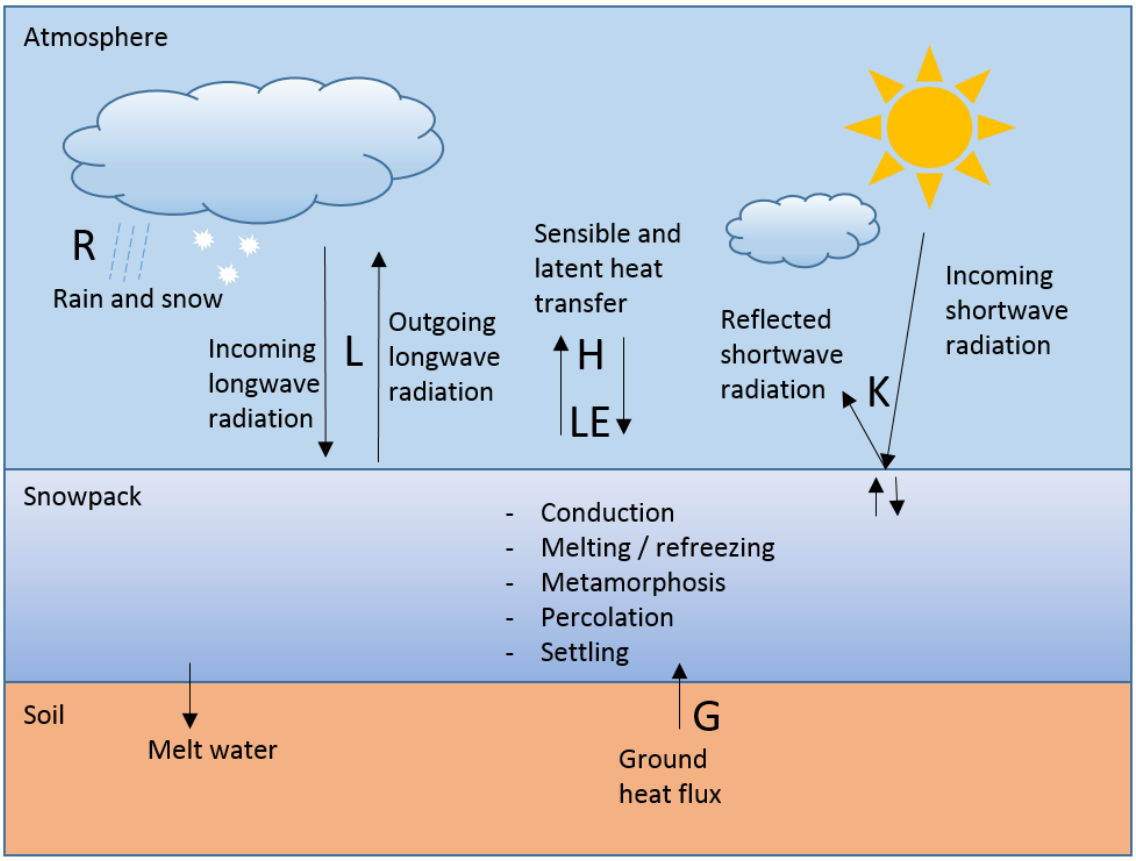

Figure 2. Mass and energy fluxes contributing to net energy exchange of the snowpack (Adapted from Pomeroy and Brun 2001).

The net energy exchange to the snowpack can be expressed mathematically as sum of the different components (Dingman 2008) as:

$$S = K + L + H + LE + R + G \tag{2}$$

where S is the net energy input to the snowpack

K is the net shortwave radiation

L is the net longwave radiation

H is the turbulent/convective exchange of sensible heat

LE is the turbulent/convective exchange of latent heat

R is the heat content of the precipitation

G is the conductive exchange of sensible heat with the ground.

The incoming shortwave radiation (SWR) is a sum of the direct and diffuse sunbeam. It is depending on the latitude, day of the year, slope inclination and aspect, cloud cover and canopy of the forest. Part of the shortwave radiation is reflected back to the atmosphere

from the surface layer of the snowpack, depending on the albedo. The net SWR is the difference between incoming and reflected shortwave radiation.

Electromagnetic energy from atmosphere, canopy cover and clouds is called longwave radiation (LWR), which can be calculated using Stefan–Boltzmann equation. It is proportional to the emissivity of the material and the temperature of the material to the fourth power. The net longwave radiation is the difference between incoming LWR and the LWR originated from snowpack. The reflected longwave radiation is negligible, since the reflectivity of longwave radiation is close to one.

2.4.2 Main phases of snowmelt

The melting period of snow can be divided into three main phases according to Dingman (2008, p. 185-189): the warming phase, the ripening phase and the output phase. The phases are usually overlapping due to the fluctuations in the air temperature and net energy flux between the snowpack and the environment. However, it is useful to use the division to understand the processes in the melting snowpack.

The warming phase begins when the net energy flow to the snowpack is positive and the snow starts to warm up towards the isothermal melting point, i.e. 0 °C. According to e.g. Dingman (2008) the amount of energy needed to reach the isothermal condition, i.e. the cold content, can be calculated with equation (2):

$$Q_{cc} = -c_i \times \rho_w \times h_m \times (T_{sp} - T_m) \quad (3)$$

where Q_{cc} is the cold content (J m^{-2})
c_i is the heat capacity of ice (J kg^{-1} K^{-1})
ρ_w is the density of water (kg m^{-3})
h_m is the snow water equivalent of the snowpack (m)
T_{sp} is the average temperature of the snowpack (K)
T_m is the melting temperature of snow (K).

At the time when the temperature of the snowpack reaches 0 °C the ripening phase begins. In temperate climates the snowpack is usually close to the isothermal state when the melt starts at the surface but in cold climates the melt-refreeze cycle can be significant, i.e. the

melt of the snowpack forms a diurnal cycle where the energy deficit must be first compensated before melt continues (Pomeroy and Brun 2001). Ripening phase continues until the amount of meltwater exceeds liquid water retention capacity (LWRC) of the snowpack. Kuusisto (1984, p. 71) found that the ripening phase can be several days long even in a shallow snowpack. The liquid water retention capacity can be calculated with equation (4) and the energy needed in ripening phase with equation (5).

$$h_{wret} = \theta_{ret} \times h_s \tag{4}$$

where h_{wret} is the water retention capacity (m)
θ_{ret} is the maximum volumetric water content (approx. ≤ 0.05)
h_s is the snowpack depth (m).

$$Q_{lwhc} = h_{wret} \times \rho_w \times \lambda_f \tag{5}$$

where Q_{lwhc} is the energy needed to satisfy the LWRC (J m^{-2})
ρ_w is the density of water (kg m^{-3})
λ_f is the latent heat of melt (J kg^{-1}).

The ripe snowpack is not capable of holding any more meltwater formed by the energy input to the snowpack. The excess water starts to percolate through the snowpack drawn by the force of gravity, eventually producing outflow from the snowpack. (Dingman 2008) The energy needed to completely melt the ripe snowpack can be calculated as:

$$Q_{melt} = (h_m - h_{wret}) \times \rho_w \times \lambda_f \tag{6}$$

where Q_{melt} is the energy needed in output phase (J m^{-2})
ρ_w is the density of water (kg m^{-3})
λ_f is the latent heat of melt (J kg^{-1}).

The amount of meltwater (SWE_m) can be calculated with equation (7) according to Pomeroy and Brun (2001):

$$SWE_m = \frac{S - Q_{cc}}{\rho_w \times L_f \times B} \quad (7)$$

where S is the net energy input to the snowpack (J m^{-2})

Q_{cc} is the cold content of the snow (J m^{-2})

ρ_w is the density of water (kg m^{-3})

L_f is the latent heat of fusion (J kg^{-1})

B is the fraction of ice in a unit mass of wet snow, often 0.95 – 0.97.

2.5 Measurement methods

Precipitation of snow can be measured with collecting gages, where the collected snow is melted and the quantity of meltwater is recorded. There are many difficulties with this method. The biggest problem is the wind which is preventing the snow to accumulate to the gage. The snow can also accumulate on the top edges of the gage which causes uncertainty. A correction factor is needed to correct the error. (Dingman 2008, p. 169) Alternative method include snow plates, snow pillows and stake stations (Kuusisto 1984 p. 12).

The development of remote sensing has opened new possibilities of precipitation measurement, the latest being Global Precipitation Measurement (GPM) satellite mission, co-led by NASA and JAXA, which was launched on February 27th, 2014. GPM provides e.g. intensity and variability of precipitation, microphysics of the ice and liquid particles within clouds and amount of water falling to Earth's surface approximately every three hours between latitudes from 65° N to 65° S. (NASA 2012)

The accumulated snowpack depth can be measured with snow stakes, which are simple rulers set through the snowpack (Kuusisto 1984, p. 12). Electronic instruments include e.g. acoustic measurement sensors, which measure the distance between the surface of the snowpack and the sensor with ultrasonic waves (Campell Scientific 2011).

Information of the areal snow cover can be obtained from snow courses, which are designed to give representative (e.g. topography, vegetation) picture of the snowpack in

the measured region. Typical snow course lengths in Finland are 2.5 km and 4 km with 50 m snow depth measurement interval. The density and water equivalent of the snowpack are determined in 8-10 measurement points on the snow course by taking snow cores with a snow tube. The snow core is taken by pushing the snow tube vertically through the snow to the ground and lifting the tube from the snowpack by simultaneously securing that the snow stays in the tube with a shovel or similar suitable tool. (Kuusisto 1984, p. 8; Dingman 2008, p. 174)

Remote sensing using satellite imagery on visible, infrared and microwave frequencies can be used to determine the areal extend of the snow cover and snow water equivalent over large areas, because the properties of snow are different than the other natural surfaces. The spatial resolution of the images is varying from tens to thousands of meters and the observation frequency of the images varies from one day to weeks. In visible and infrared bands the cloud cover is hindering the observations and additionally in infrared band it's sometimes hard to distinguish the snow cover from the other surfaces as the temperatures can be close to each other. (DeWalle and Rango 2011, p. 122-125)

As an example of remote sensing data a visible image of fractional snow cover (FSC) in Northern Finland on 28th of May 2014 is presented in Figure 3. The image is generated by Finnish Environment Institute (SYKE 2014) based on Terra MODIS spectroradiometer (NASA) satellite observations in approximately 500 m x 500 m resolution.

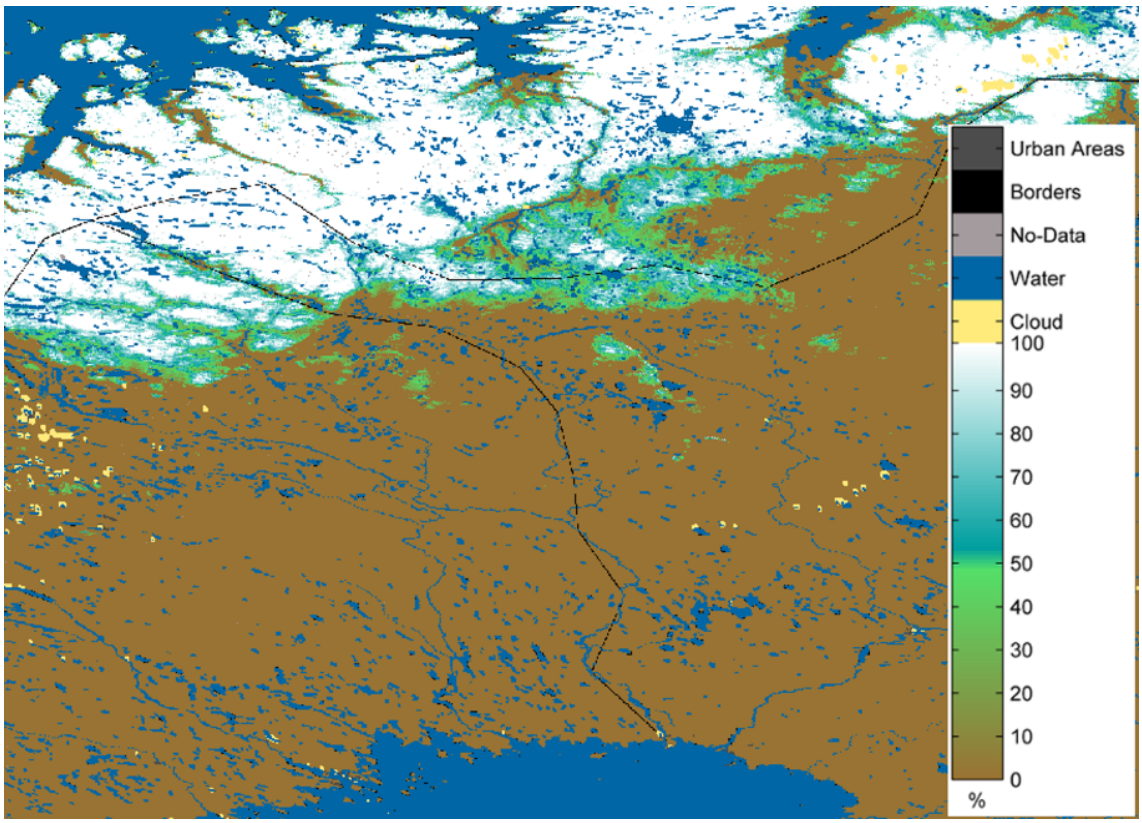

Figure 3. Fractional Snow Cover in Northern Finland on 28th of May, 2014. Colors from brown to white correspond to FSC of 0-100%. Water and cloud areas are shown with blue and yellow color, respectively. Resolution of the image is approximately 500 m x 500 m. Figure modified from an image generated by Finnish Environment Institute (SYKE 2014).

2.6 Snow modelling

Numerical modelling can be used to study the development of the snowpack and its structure (Rasmus 2005, p. 123) and parameters affecting the snowpack. In hydrology the purpose of a snow model is usually to predict the runoff generated by the snowpack. Such models are called snowmelt-runoff models. The models can be classified to either deterministic or stochastic and either lumped-parameter or distributed. Deterministic models give a single value of outflow for a constant set of input variables. The input for stochastic model is a statistical distribution of the input variables and it gives a range of outflow. Lumped-parameters or point models handle the basin as homogenous area whereas in distributed models the catchment is divided into sub basins. (DeWalle and Rango 2011, p. 266)

The deterministic point models include empirical degree-day models, also called as temperature index models, and snowpack energy-balance based physical models. Some of the models include also the internal snowpack structure. (Rasmus 2005, p. 125)

Empirical degree-day models are based on a relationship between difference of positive air temperature, melt temperature and the melt rate, represented by a degree-day factor (Kuusisto 1984, p. 35). According to Kuusisto (1984, p. 90) the advantages of using air temperature in as the predictor for snowmelt are the simplicity and its nature of integrating heat energy into one parameter. Disadvantages include that compared to radiation, wind and humidity the air temperature is a secondary meteorological variable. The simplest mathematical expression for the model is

$$M = DDF \times (T_a - T_m) \tag{8}$$

where M is the amount of snowmelt (mm d^{-1})
DDF is the degree-day factor (mm $°C^{-1}$ d^{-1})
T_a is the daily mean air temperature (°C)
T_m is the threshold temperature for snowmelt (°C).

The air temperature is rather easily available making the degree-day model a convenient method in snowmelt calculations. Even though the degree-day model is usually less accurate than physically based models it can often outperform the energy-balance models in catchment scale when estimating the snowmelt (Hock 2003, Vehviläinen 1992). Hock (2003) points out two shortcomings of temperature index models: 1) the accuracy is decreasing with increased temporal resolution and 2) accuracy of spatial variability is low because of possible differences in melt rates in variable vegetation and topography e.g. changes in shading, slope and aspect. Impact of the topography and vegetation can be estimated by a relationship found in a study by Eggleston et al. (1971), cited by Gray (1981, p. 418). This relationship includes fraction of forest cover, slope factor for solar radiation and albedo as parameters for the degree-day factor.

Physical models are usually more accurate than the temperature index models. They are based equations derived from the physical principle of conservation of the energy, as described in chapter 2.4 and equation (2). The intense data requirements can be considered as the downside, as the modelling requires air temperature, wind speed, humidity, cloud cover, precipitation, snow-surface temperature and short and longwave radiation data (Dingman 2008, p. 210).

Examples of advanced physical snow models include SNOWPACK developed at the Swiss Federal Institute for Snow and Avalanche Research (SLF 2015), CROCUS developed in French National Centre for Meteorological Research by the Research group of atmospheric meteorology (CNRM-GAME 2015) and ESCIMO.spread, developed in the Institute of Geography at the University of Innsbruck by the Alpine Hydro Climatology research team (AHC 2015).

3 STUDY AREA

3.1 Fell area

The study area is located in Northern - boreal subarctic region in Pallas - Ylläs National Park in north-western Finland (Figure 4). Locations of the measurement plots are on the Sammaltunturi and Mustavaara fells, which are shaped during the Pleistocene glaciations (Sutinen et al. 2009; Liwata et al. 2014). The forest in the area is mainly Norway spruce including occasional Scots pine. Downy and mountain birch are also observed, especially closer to the transition region on the slopes.

3.2 Measurement plots

Three of the measurement plots are located on the southwest slope of the Sammaltunturi, ST2 in spruce forest and ST3 at the tree line whereas ST4 is situated on the open slope above the tree line (Figure 4). Elevations of the sites are 400 m, 450 m and 475 m a.s.l, respectively. GTK measurement site GC7 is situated adjacent to ST2 and GC4 close to ST3. ST5 is on the southern slope of Mustavaara, close to the bare fell peak at the elevation of 480 m a.s.l. ST6 is placed on an open mire northeast from Mustavaara at elevation of 375 m a.s.l and ST7 in spruce forest at the northeastern slope of Mustavaara at elevation of 380 m a.s.l. Each of the test plots included 5 measurement points with approximately 10 - 50 m distance from each other. Sample pictures from each test plot are presented in Figure 5 and geographical locations of the plots are depicted in Figure 4, which includes also a more detailed exposition of measurement plot ST3. Finnish Meteorological Institute has several measurement stations at the near area (Figure 4). The tabulated environment and topography details are presented in Table 1. The topography details (Altitude, Inclination and Aspect) are extracted from a digital elevation model (DEM) produced by the National Land Survey of Finland.

Table 1. Environment and topography details of the measurement and reference sites. Inclination is the steepness and aspect the orientation of the fell slope. Aspect factor is defined by the orientation of the slope which controls the amount of solar radiation received by the slope, 1 = south and 8 = north.

Site	Environment	Altitude (masl)	Inclination (degrees)	Aspect (degrees)	Aspect factor
ST2 / GC7	spruce forest	400	5	240	2
ST3 / GC4	tree line	450	5	220	2
ST4	open slope	475	4	270	4
ST5	next to bare fell	480	5	170	1
ST6	open mire	375	1	70	5
ST7	spruce forest	380	6	45	7

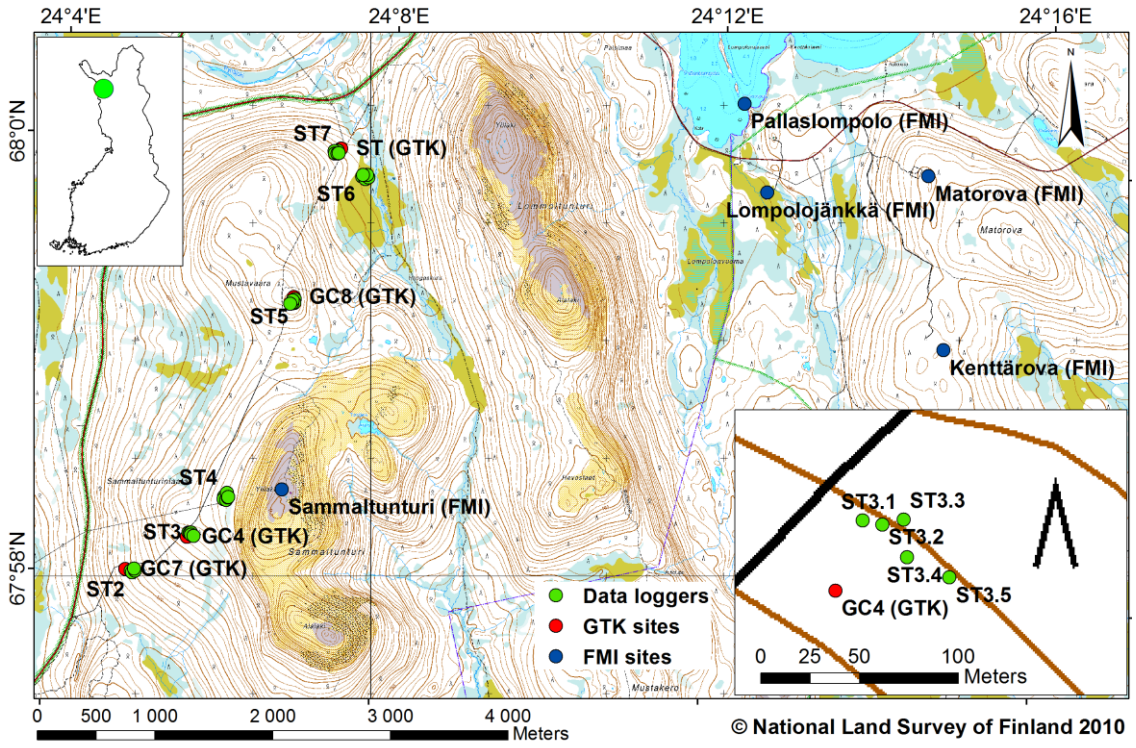

Figure 4. Fell area of Sammaltunturi and Mustavaara including test plots and GTK reference sites. Also FMI measurement sites are included in the figure. The lower right corner presents a more detailed picture of test plot ST3.

Figure 5. Test plots at Sammaltunturi and Mustavaara.

3.3 Climate

According to Köppen - Geiger climate classification the study area belongs to class Dfc, cold climate without dry season and cold summers (Peel et al. 2007). The annual mean temperature in the period of 1981 - 2010 in the area was -2 - -1 °C whereas annual precipitation amounted of 500 – 550 mm (Pirinen et al. 2012). The seasonal average precipitation during the period of 1981 - 2010 in the area falls in the range of 140 - 150 mm in fall, 90 - 100 mm in winter, 90 - 100 mm in spring and 200 - 210 mm in summer (FMI 2015).

Average ranges of starting and ending date of permanent snow cover during the period of 1981 - 2010 were 17.10. – 27.10. and 10.5. – 20.5., respectively, corresponding to 205 – 225 days of snow pack. The thickest snow cover usually takes place in early April. (FMI 2015) The average maximum annual snow water equivalent range during period of 1971 – 2000 was 200 – 240 mm (Veijalainen et al. 2012).

The nearest snow courses of the research area are shown in Figure 6 and the measurement data is presented in Table 2. Precipitation and temperature data used in snow model is received from the FMI Kenttärova measurement site, which is included in Figure 6. The measured precipitation during the study period at Kenttärova site was 138.5 mm in autumn, 114.3 mm in winter and 125.1 mm in spring, which is total of 377.9 mm during the hypothetical snow season.

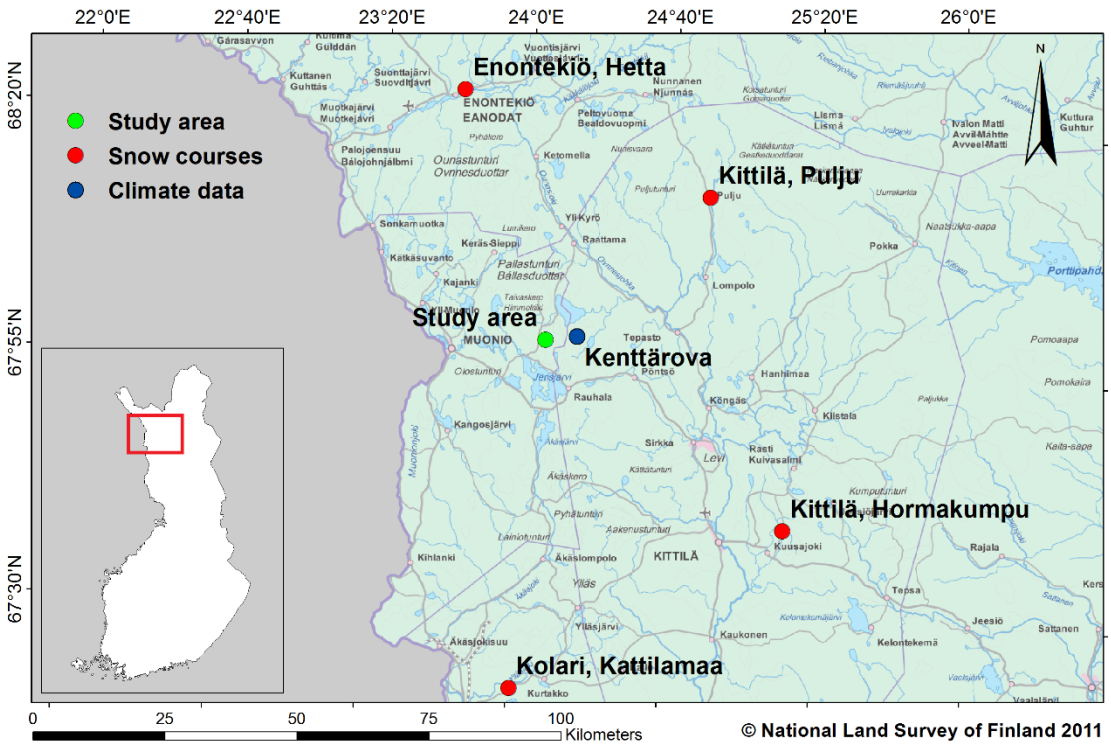

Figure 6. Locations of SYKE snow courses. FMI observation site for precipitation and temperature which were used as input in snow model.

Table 2. SYKE snow course SWE measurements from winter 2013 – 2014 in the experiment region. The unit of the measurements is mm.

Date	Kittilä, Hormakumpu	Enontekiö, Hetta	Kittilä, Pulju	Kolari, Kattilamaa
11/2013	22	NA	14	24
12/2013	68	71	58	45
01/2014	92	NA	115	83
02/2014	134	NA	139	107
03/2014	147	NA	181	128
04/2014	92	113	193	117
05/2014	60	NA	NA	NA

4 METHODS AND MATERIALS

4.1 Snow temperature measurements

The snowpack temperature was measured using Onset Hobo Pendant Temperature Data Logger 8K model UA-001-08 (Figure 7). With the 8K model approximately 6500 measurements can be recorded. Operating range of the sensor in water/ice is from -20°C to 50°C with accuracy of ±0.53°C from 0° to 50°C. Resolution is 10 - bit, which equals to 0.14°C at 25°C and the response time of the sensor is 5 - 10 minutes. (Onset 2015)

Figure 7. HOBO Pendant® Temperature/Alarm Data Logger 8K - UA-001-08.

Temperature sensors were programmed to start recording on 18th of April 2014 at 12:00. 15 minutes logging interval was used. The sensors were protected with a rubber cover to avoid possible harm to the circuit board by UV-radiation.

Loggers were installed on the ground and at fixed height of 30 cm (Figure 8) in five adjacent locations in six test plots on 16 - 17th of April 2014 (Figure 4). Constant height of the upper logger was secured by attaching it to a wooden stick, which was set to stand

on the ground. The pit in the snowpack was kept as small as possible to minimize the disturbance of the snow. A small cavity was made on the wall of the pit where the sensors were placed and carefully pushed to the snowpack. The snow which was dug from the pit was finally shoveled back to the pit, but it only filled the hole to approximately 50 - 60% level. Additional snow needed to be fetched to fill the hole completely, which increased the density of the snowpack. After the snow was melted from the test area the loggers were collected on 17 - 18th of June 2014.

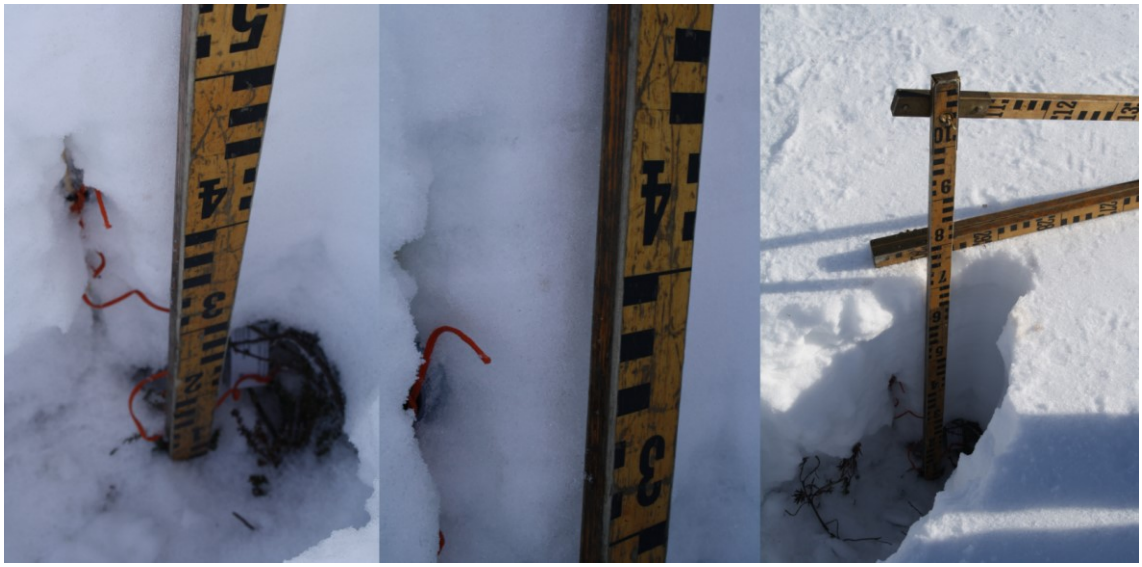

Figure 8. Installation of the temperature loggers (Pictures: Pertti Ala-aho).

4.2 Temperature logger data

It was noticed during the temperature data extraction from the loggers that some of them had problems during the measurement. The number of functioning loggers for each site and height is presented in Table 3.

Table 3. Number of data loggers out of five for each site and height.

Height \ site	ST2	ST3	ST4	ST5	ST6	ST7
30 cm	4	5	4	5	4	4
0 cm	5	3	5	5	5	5

Temperature data from the loggers at test site ST2.1 is presented in Figure 9. The measurement period was from 19th of April 2014 to 15th of June 2014 with measurement interval of 15 minutes. It can be seen from the graph that the snow pack temperature stays

at 0°C from the ground up to 30 cm over half of the measurement period. The temperature of the upper logger starts fluctuating first, followed by the fluctuation of the temperature of the sensor on the ground few days later.

Air temperature in sites ST4, ST6 and ST7 was measured using Hobo Pendant Temperature Data Loggers by attaching the logger at height of approximately 2 m to a tree and covering it with a shed to protect the sensor from solar radiation. At sites ST2 and ST3 the air temperature from GTK reference sites GC7 and GC4 was used. Air temperature was unavailable at site ST5 and temperature from site ST4 was used because the matching altitude of the sites.

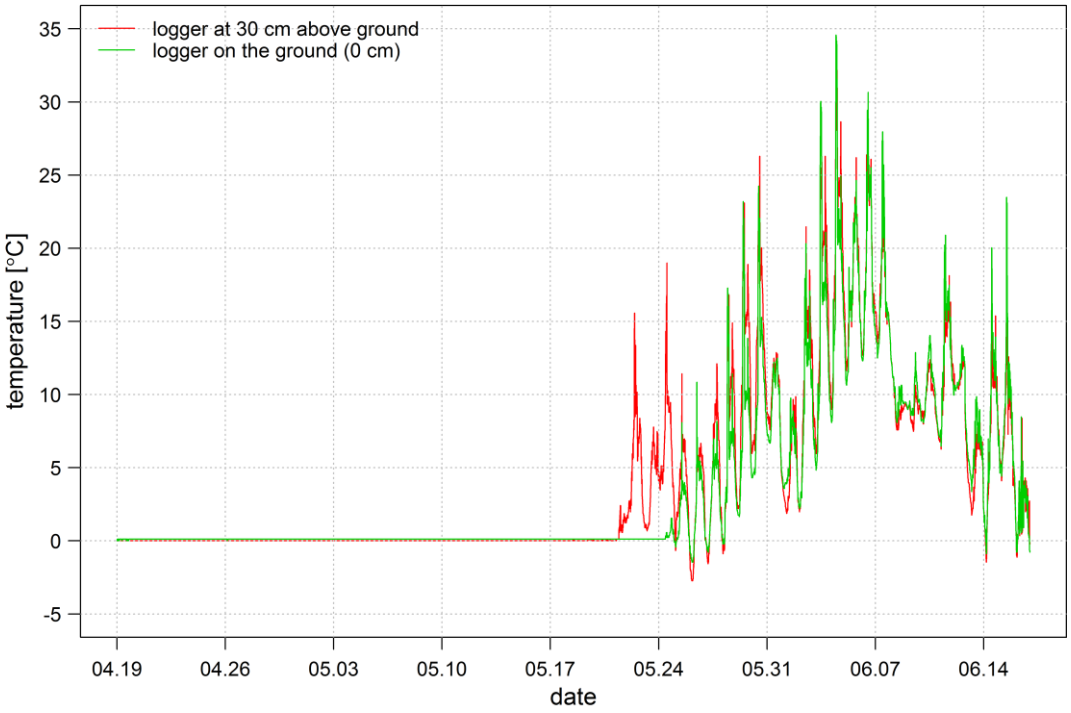

Figure 9. Raw temperature data from spruce forest point ST2.1 from experiment period from 19th of April 2014 to 15th of June 2014.

Period of one week from 20 to 27th of May 2014 of the logger temperatures and the air temperature at ST2.1 is presented in Figure 10. It can be seen from the figure that at point 3 the logger at 30 cm above ground and at point 5 the logger on the ground starts to follow the air temperature. Peaks in sensor temperatures can be seen around midday, assumed to be caused by solar radiation penetrating the snowpack.

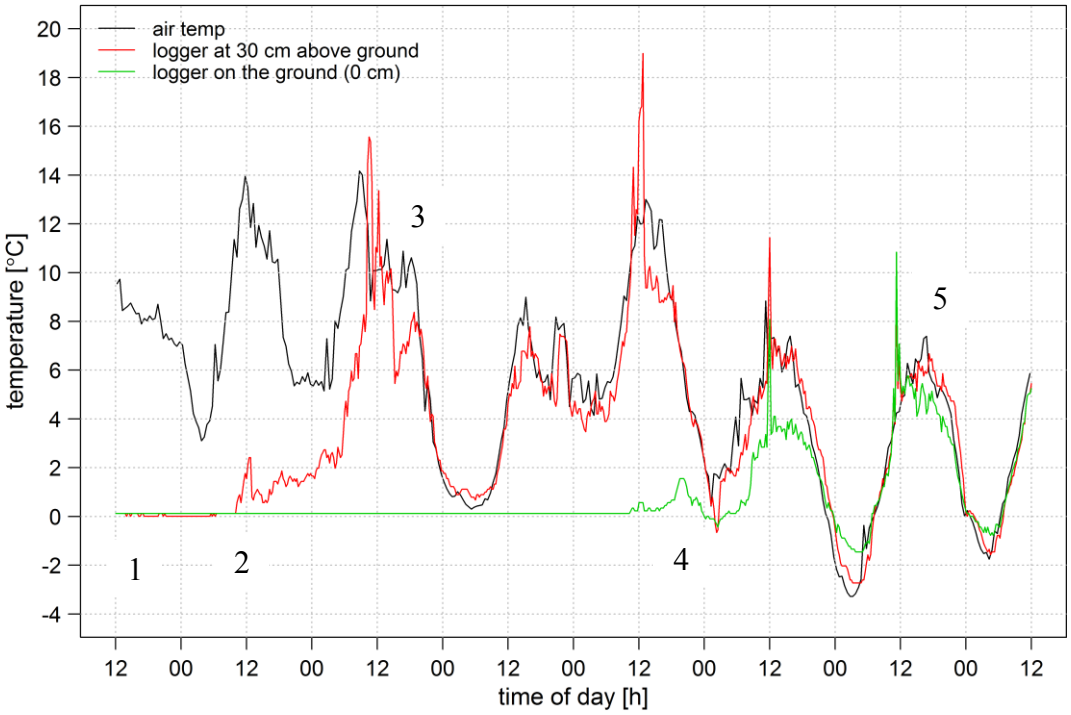

Figure 10. Example air (black), logger at 30 cm (red) and logger on the ground (green) temperatures as a function of time in forest site ST2.1 from 20th to 27th of May 2014. At point 1 both of the loggers are still assumed to be covered in snow as the temperature is constant 0°C. At point 2 (21st of May) the temperature of the upper sensor starts to rise because the insulating effect of snow above the sensor has decreased. The upper sensor is assumed to be free of snow at point 3 (22nd of May) as the temperature starts to follow the air temperature. At point 5 (26th of May) the logger on the ground is assumed to be free of snow.

Removing the assumed impact of the solar radiation peaks to the logger temperatures was done with an algorithm (Eq. 9) which cuts the temperature of the sensor T_{logger} to the air temperature T_{air} when the sensor temperature is higher than air temperature and the air temperature is higher than 0.2 °C. Smoothened data for ST2.1 is presented in Figure 11. The smoothened data is used in the following parts of this study.

$$T_{logger} = \begin{cases} T_{air}, & when\ T_{logger} > T_{air}\ and\ T_{air} > 0.2\ °C \\ T_{logger}, & when\ T_{logger} \leq T_{air} \end{cases} \quad (9)$$

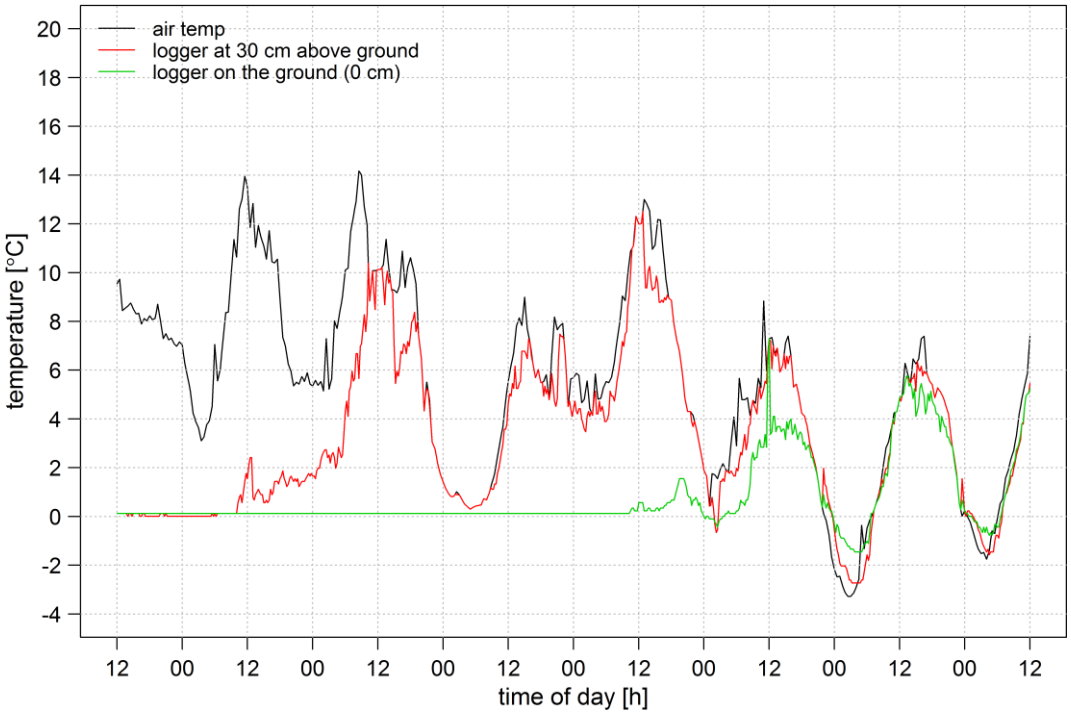

Figure 11. Example raw air (black), logger at 30 cm (red) and logger on the ground (green) temperatures as a function of time in forest site ST2.1 from 20th to 27th of May 2014. Peaks removed with algorithm (Eq. 9).

Diurnal standard deviation (SD) of smoothened temperature of each logger in the snow pack was calculated from the measurements at 15 min interval, equaling to 96 daily measurement points. The calculated SD was used to determine the date when the loggers were free of snow (Reusser and Zehe 2011). The threshold value for standard deviation of the sensor temperature was selected to be 2.0, i.e. the logger is assumed to be free of snow when the daily standard deviation is above the threshold value.

GTK reference measurement stations GC7 and GC4 (Figure 12) were used to verify the results at ST2 and ST3. The stations are equipped with SR50A SONIC RANGING SENSOR by Campbell Scientific, Inc. (Figure 12). The measurement range is from 0.5 to 10 m with accuracy of ±1 cm or 0.4% of the distance to the target. Resolution of the sensor is 0.25 mm. The speed of sound varies with the air temperature, therefore the sensor readings are compensated using the air temperature measurements and an equation provided by the device manufacturer. (Campell Scientific 2011)

Figure 12. GTK measurement station GC7. SR50A SONIC RANGING SENSOR in small picture on the right.

4.3 Snowpack measurements and canopy cover estimation

The snow melt processes and rates are affected by the distribution and metamorphosis of the snow pack during the accumulation period (Kuusisto 1984, p. 28). To determine the physical state and the variability of the snow at the study sites before the melt period the snowpack height and density were measured 16 - 17th of April 2014. This was done by taking snow cores from the points where the temperature sensors were mounted. Snow water equivalent was calculated using the measured parameters (Table 4). Snow depth values at 16th of April at GTK reference measurement stations GC4 (Figure 12) and GC7 are included in Table 4. All measurement results from each ST site can be found from Annex 1.

Table 4. Average snow depth, density and snow water equivalents at test plots on 16 - 17th of April 2014. Snow depths at GTK reference sites at on 16th of April 2014.

Site	Environment type	Snow depth (m)	Snow density (kg m^{-3})	SWE (mm)
ST2	spruce forest	0.79	287	227
ST3	tree line	0.91	290	265
ST4	open slope	0.83	306	256
ST5	next to bare fell	0.89	322	289
ST6	open mire	0.81	280	229
ST7	spruce forest	0.89	271	241
GC4 (ST3)	tree line	0.88	NA	NA
GC7 (ST2)	spruce forest	0.68	NA	NA

The canopy coverage of test each test point was approximated from digital camera pictures (Korhonen and Heikkinen 2009; Jonckheere et al. 2005) taken when the temperature loggers were fetched from the field on 17 - 18th of June. There was some leaves already in deciduous trees which affect the accuracy of the canopy coverage determination. The camera was set pointing at the sky on the surface of a plate placed on the ground. A spirit level was used to ensure that the camera was pointing at the zenith. Two pictures were taken at each test site, by turning the camera 90 degrees horizontally between the shots. Image manipulation program (GIMP 2015) was used to determine the percentage of canopy by using a threshold tool to separate the brighter blue sky and darker canopy parts in the pictures as white and black (Figure 13). After this the histogram info of the picture was used to determine the number black pixels, which represent the canopy. Average canopy determined from the two pictures taken at each test point was finally used. The determined canopy coverages are shown in Table 5.

Figure 13. Canopy coverage percentage determination example, ST2.1. Original picture on the left. Threshold tool in GIMP (2015) applied on the right.

Table 5. Determined canopy coverages in percentages at each test point.

Site\Point	1	2	3	4	5	Mean
ST2	23.0	21.3	26.7	3.8	10.6	17.1
ST3	4.6	15.7	5.2	4.3	1.3	6.2
ST4	0	0	0	0	0	0
ST5	0	1.9	3.6	0	19.8	5.1
ST6	0	0	0	0	0	0
ST7	14.0	0	45.5	13.7	34.6	21.6

Non-parametric Kendall correlation test was used to analyze the interrelations of the measured snow properties and their relations to topography and canopy coverage at the study area. Kendall tau measures the monotonic relationship between the variables and is rank-based, therefore resistant to outliers. Function cor.test in R software (R Core Team 2014) was used to calculate the Kendall tau and its p-value describing the strength of the calculated relation. Normally an exact p-value is calculated for small data sets. If the data set contains tied pairs, which is often the case in this study, a large sample approximation with adjustment for ties is used. In this case the test statistic is approximated by a normal distribution. The existence of ties in small sample size introduces uncertainty as with small sample sizes only exact test provides accurate results for the p-value. However, the p-values for Kendall tau calculated using large sample approximation are very near to the exact values also for small samples sizes. (Helsel and Hirsch 2002; R-manual 2015)

4.4 Temperature-degree factors

To estimate the snowmelt rates in experiment plots temperature-degree factors were calculated. Snowpack heights of 300 mm (h_s) and 0 mm (h_0) are assumed when the logger at 30 cm height and on the ground are free of snow, respectively. The corresponding dates are designated as t_{30} and t_0 and t_{melt} as the time as days between t_{30} and t_0. The mean air temperature (T_{air_mean}) is calculated for a period of time from t_{30} and t_0. Snowpack density (δ_s) was assumed to be 329 kg m^{-3} in forest and 349 kg m^{-3} in open areas (Kuusisto 1980, p. 69), because densification of snowpack was assumed after the field measurements on 16 - 17th of April. Water density (δ_w) of 1000 kg m^{-3} was used. The threshold for snowmelt (T_m) was estimated to be 0 °C. Combining equations (1) and (8) the degree day factors can be calculated with equation (10).

$$DDF = \frac{h_s \times \frac{\delta_s}{\delta_w}}{t_{melt} \times (T_{air\_mean} - T_m)} \tag{10}$$

Kuusisto (1984, p. 97) presented empirical equations (11 and 12) for relationship between snow density (ρ_s) and degree day factors for open field (DDF_o) and forest (DDF_f). The DDFs calculated with the equations were utilized for comparison with the snowmelt modelling results obtained with degree-day factors determined using the temperature loggers.

$$DDF_o = 0.00196 \times \rho_s - 2.39 \tag{11}$$

$$DDF_f = 0.00104 \times \rho_s - 0.70. \tag{12}$$

4.5 Degree-day snow model

To test and verify the validity the determined melt rates and the moment when liquid water is released as outflow from the snowpack an empirical degree-day model was employed. A model presented by DeWalle and Rango (2011, p. 279 - 284) was selected because it includes estimations for cold content and liquid water holding capacity, which are used to determine the critical moment for outflow from the snowpack, i.e. the time when snowpack is ripe and it contains maximum amount of liquid water. Fundamentally

the model is a based on the principle of mass conservation. Mass-balance of the water in the snow pack over a given time period is calculated as

$$\Delta SWE = P \pm E - O \tag{13}$$

where ΔSWE is the change in snow water equivalent over a given time period (mm)
P is the precipitation as rainfall and snowfall (mm)
E is the net vapor exchange between the snowpack and environment (mm)
O is the liquid water outflow from the snowpack (mm).

The model used in this study neglects the net vapor exchange between the snowpack and the environment, which can be significant in dry and windy climates especially when the solar radiation is high. Routing for liquid water in the snowpack is not included as it is assumed that liquid water stays in the snowpack. The lag of transmission of liquid water through the snowpack is neglected as well as the melting of the snow due to heat in the liquid precipitation.

The structure of the model is presented in Figure 14. The precipitation type is determined using air temperature (chapter 4.5.1). Melt is calculated with the degree day equation (chapter 4.5.2). Three types of storages are introduced as snow water equivalent (SWE), cold content (CC) and liquid water holding capacity (WHC) which are calculated for the given period of time, i.e. time step, to finally determine the outflow. Storages are described in more detail in chapters 4.5.3 – 4.5.5. The goodness of the model is evaluated using coefficient of determination and root mean squared error (chapter 4.5.6). Model was programmed and ran using R software. The time step for the calculations was defined as one day.

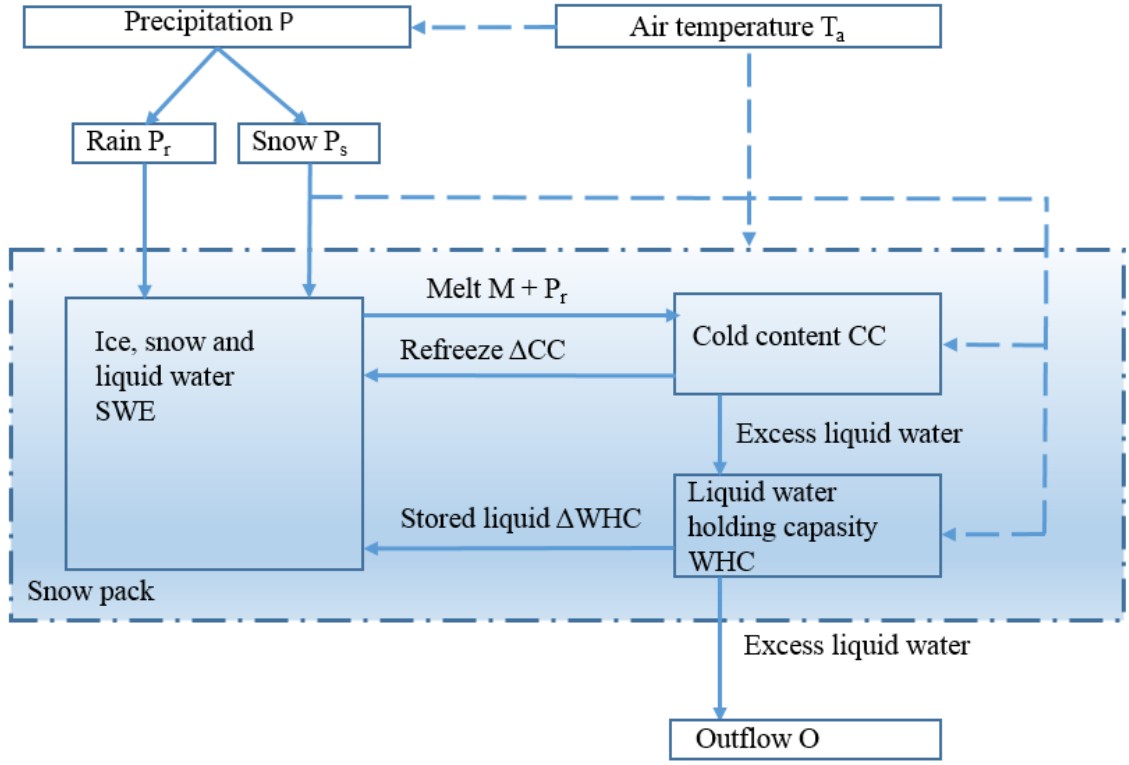

Figure 14. Snow model for accumulation and melt periods.

Four types of main events are separated in the model, depending on the air temperature (T_a), critical temperature for snow fall (T_{crit}), temperature threshold for snowmelt (T_m) and amount of precipitation (P).

1) P > 0 and $T_a > T_{crit}$ (Rainfall). Precipitation is rainfall (P_r), melting (M) is computed depending of the melt threshold temperature (T_m) and air temperature (T_a). Rain and melt together are calculated as potential snowpack outflow.
2) P > 0 and $T_a <= T_{crit}$ (Snowfall). Precipitation is snowfall (P_s) and snow water equivalent (SWE) is increased by the amount of (P_s). Cold content (CC) is incremented depending on the snowpack surface temperature (T_s) and air temperature (T_a). Water holding capacity is incremented relatively to P_s. Melt (M) is computed depending of the T_m and T_a and it becomes potential outflow.
3) P = 0 and $T_a > T_m$ (Melt). No precipitation occurs and air temperature (T_a) is greater than temperature for melt (T_m). Melt (M) is calculated and it becomes potential outflow from the snowpack.
4) P = 0 and $T_a <= T_m$ (No Melt). No precipitation occurs and air temperature (T_a) is smaller or equivalent to melt temperature (T_m). Cold content (CC) is adjusted depending on the snow pack surface temperature (T_s) and air temperature (T_a).

4.5.1 Precipitation

The precipitation as well as the air temperature data used in the model are from the Finnish Meteorological Institute (FMI) measurement site Kenttärova (Figure 6). The form of precipitation can vary between solid and liquid, as described in chapter 2.3. In this model the precipitation is either snow or rain, depending on the air temperature T_a and the threshold temperature T_{crit}. Because of the possible errors in precipitation measurements, described in chapter 2.5, the measurements must be calibrated using a correction factor. The corrected daily snow and rain precipitation are calculated as:

$$P_s = P \times CF_s, when\ T_a \leq T_{crit} \tag{12}$$

$$P_r = P \times CF_r, when\ T_a > T_{crit} \tag{13}$$

where P_s is the corrected snow precipitation (mm d^{-1})
P_r is the corrected liquid precipitation (mm d^{-1})
P is the measured precipitation (mm d^{-1})
CF_s is the correction factor for snow precipitation
CF_r is the correction factor for liquid precipitation
T_a is the mean daily air temperature (°C)
T_{crit} is the calibrated critical temperature for snowfall (°C).

4.5.2 Snow melt

The melt for each time step is calculated with degree-day model presented as equation:

$$M = \begin{cases} DDF \times (T_a - T_m), & \text{when } T_a > T_m \\ 0, & \text{when } T_a \leq T_m \end{cases} \tag{14}$$

where M is the amount of snowmelt (mm d^{-1})
DDF is the degree-day factor (mm $°C^{-1}$ d^{-1})
T_m is the threshold temperature for snowmelt (°C).

Even though the net vapor exchange between the snowpack and environment is directly neglected in the model it is incorporated to the degree-day factor because it integrates the heat energy allocated to the snowpack.

4.5.3 Snow water equivalent storage

The snow water equivalent storage (SWE) represents the main storage in the model. It contains all ice, snow and liquid water present in the snow pack. SWE is increased during precipitation and by increase in liquid water stored in the water holding capacity storage. The SWE is reduced by melt and rain which are drained from the snowpack after cold content and water holding capacity storages are satisfied. The equation for the computation is:

$$SWE_{\mathrm{i}+1} = SWE_{\mathrm{i}} + P_{i+1} + LWC_{i+1} - LWC_i - \left(M_{i+1} + P_{r,i+1}\right) \quad (15)$$

where SWE is the snow water equivalent of the snow pack (mm)
P is the precipitation (mm)
LWC is the amount of stored liquid water in the snowpack (mm)
M is the melt (mm)
P_r is the liquid precipitation (mm)
i is the time step (day).

4.5.4 Cold content storage

Cold content in the snowpack is calculated using empirical degree-day cold-content model presented by Anderson (1973) cited in DeWalle and Rango (2011). The model assumes that depending on the gradient between air temperature and snow surface temperature the snowpack can gain or lose energy due to heat conduction. A cold-content degree-day factor is used as the coefficient for the amount of energy exchange. According to DeWalle & Rango (2011, p. 278) the typical range of the factor is 0.2 – 0.5 mm °C d^{-1}, which is about 1/10 of the degree-day factors for snow melt. This can be explained by the insulating properties of the snowpack. When the snowpack is ripe the cold content reaches its minimum value, 0 mm. The equation for the computation of the change in cold content is:

$$CC_{i+1} = CC_i + CCF \times \left(T_{s,i+1} - T_{a,i+1}\right) \times \Delta t \quad (16)$$

where CC is the cold content (mm)

CCF is the cold-content degree-day factor (mm °C d^{-1})

T_s is the snow surface temperature (°C)

Δt is the calculation interval (d).

If the snowpack is not ripe, any occurring rain and melt is first subtracted from the snowpack cold content using equation (17). The physical explanation is freezing of the liquid water. Remaining liquid water is defined as excess liquid for filling the liquid water holding capacity.

$$CC_{i+1} = CC_{i+1} - \left(M_{i+1} + P_{r,i+1}\right) \quad (17)$$

Jordan (1991) found that snow surface temperature is highly correlated with the air temperature. The snow surface temperature required in cold content calculations is determined by temperature index method used e.g. by Marks et al. (1992):

$$T_{s,i+1} = T_{s,i} + TSF \times \left(T_{a,i+1} - T_{s,i}\right) \quad (18)$$

where TSF is the surface temperature factor.

According to DeWalle and Rango (2011) the TSF values between 0.1 (Marks et al. 1992) and 0.5 (Anderson 1973) are used. With higher TSF values the surface temperature follows more closely the air temperature. The maximum value for the snow surface temperature is 0 °C. If the snow precipitation exceeds 5 mm the surface temperature is set to air temperature because snowfall forms a new surface layer of the snowpack (Anderson 1976, cited in DeWalle and Rango 2011).

4.5.5 Liquid water holding capacity storage and outflow

Before the any liquid water can form outflow from the snowpack the liquid water holding capacity (WHC) needs to be filled. In the used model the water holding capacity is incremented during snowfall with equation:

$$WHC_{i+1} = WHC_i + (f/100) \times P_{r,i+1} \quad (19)$$

where WHC is the liquid water holding capacity of the snowpack (°C)
f is the maximum liquid water content of the snowpack (%).

During rain and melt events the excess liquid water which was not refrozen by the cold content is filling the water holding capacity and subtracted from it using equation (20). The minimum WHC is zero. The increase in liquid water content in the snowpack is presented as ΔLWC. Surplus liquid water is drained from the snowpack as outflow (O).

$$WHC_{i+1} = WHC_{i+1} - excess(M_{i+1} + P_{r,i+1}) \quad (20)$$

where WHC is the water holding capacity (mm).

4.5.6 The goodness of the model

Coefficient for determination R^2 (Eq. 21) for SWE between measured and modelled on 16th of April was used to determine the goodness of the model at the end of the snow accumulation season.

$$R^2 = 1 - \frac{\sum(y_i - \hat{y}_i)^2}{\sum(y_i - \bar{y}_i)^2} \quad (21)$$

where y_i is the measured SWE (mm)
$\hat{y}_i$ is the modelled SWE (mm)
$\bar{y}_i$ is the mean measured SWE (mm).

Root mean squared error (RMSE) was used to assess the accuracy between the modelled and measured date for end of the permanent snow cover, e.g. when all snow had melted. RMSE was calculated using equation (Hersel and Hirsch 2002):

$$RMSE = \sqrt{\frac{(y_i - \hat{y}_i)^2}{n}} \tag{22}$$

where y_i is the measured date for end of permanent snow cover

$\hat{y}_i$ is the modelled date for end of permanent snow cover

n is the number of data points.

5 RESULTS

5.1 Timing and variability of snowmelt

Average daily snowpack depth at the GTK reference site GC7, daily standard deviation of the air temperature and logger temperatures at ST2.1, which is the second closest point from GC7, during period from 19th of April to 15th of June 2014 are depicted in Figure 15. It can be seen from the figure that first the standard deviation of the temperature logger at 30 cm above the ground (red) rises sharply and after a few days the same behavior is seen in the data from logger on the ground level (green). The mean snow depth at the GTK GC7 measurement station can be seen to match reasonably well with the rise of standard deviation of ST2.1 logger temperatures. The determined variability of the snowmelt from 30 cm to 0 cm at each test plot is depicted in Figure 16.

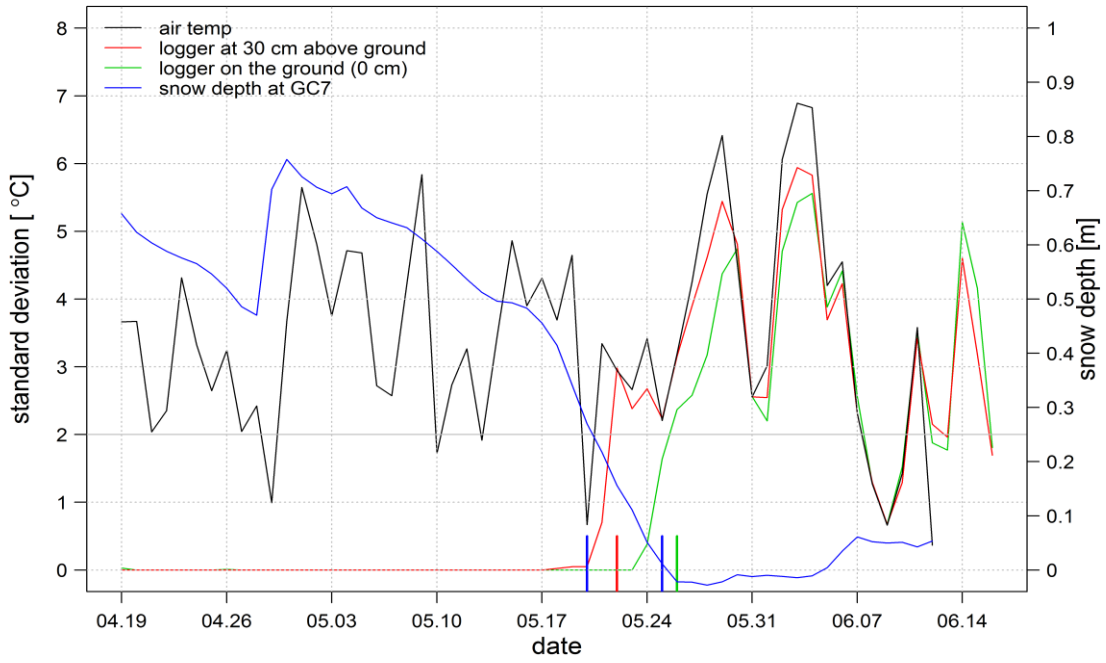

Figure 15. Diurnal SD of air temperature and the loggers in the snowpack at site ST2.1 in forest during period between 19th of April and 15th of June 2014. Snow depth at the GTK reference station GC7 is shown in blue. The determined dates for the loggers to be free of snow and respective times of snowpack depth measured by GTK are added as vertical lines at the x-axis.

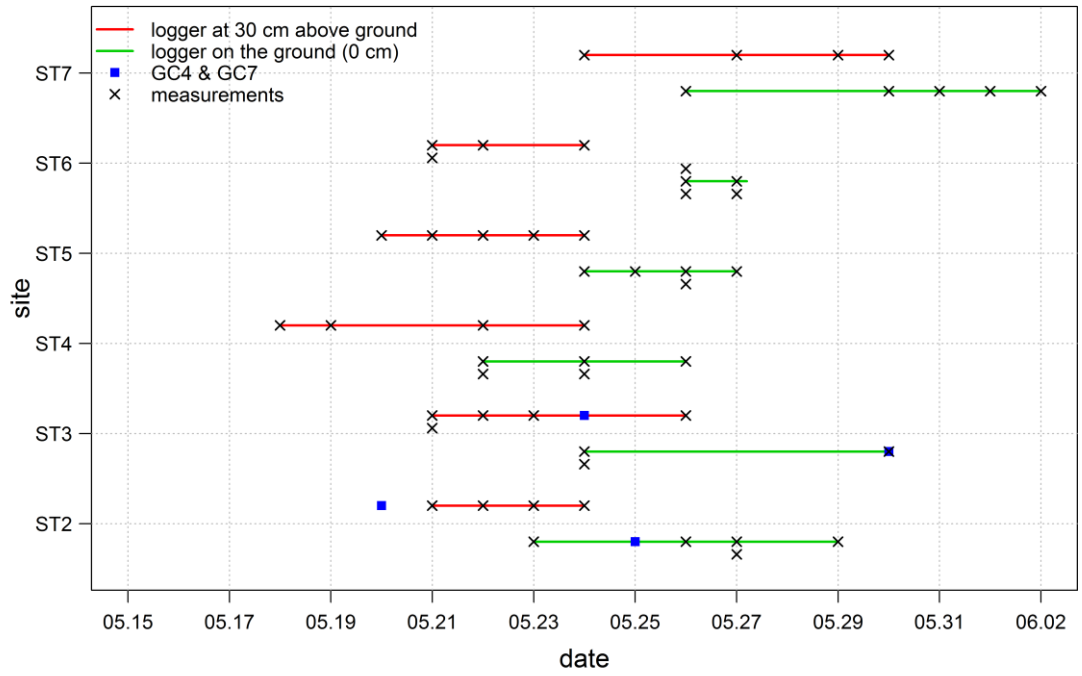

Figure 16. Measured spread for the dates when the temperature loggers are found to be free of snow in each test plot. GTK GC4 and GC7 measurement station dates for corresponding snow heights are added with blue markers.

5.2 Snowpack properties

Statistical parameters of median, minimum, maximum, first and third quartiles and coefficient of variation of the snow water equivalent, snow density and snow depth measured on 16 - 17th of April 2014 were calculated to determine the variability of the snow conditions. The results are presented as boxplots in Figure 17 and Table 6.

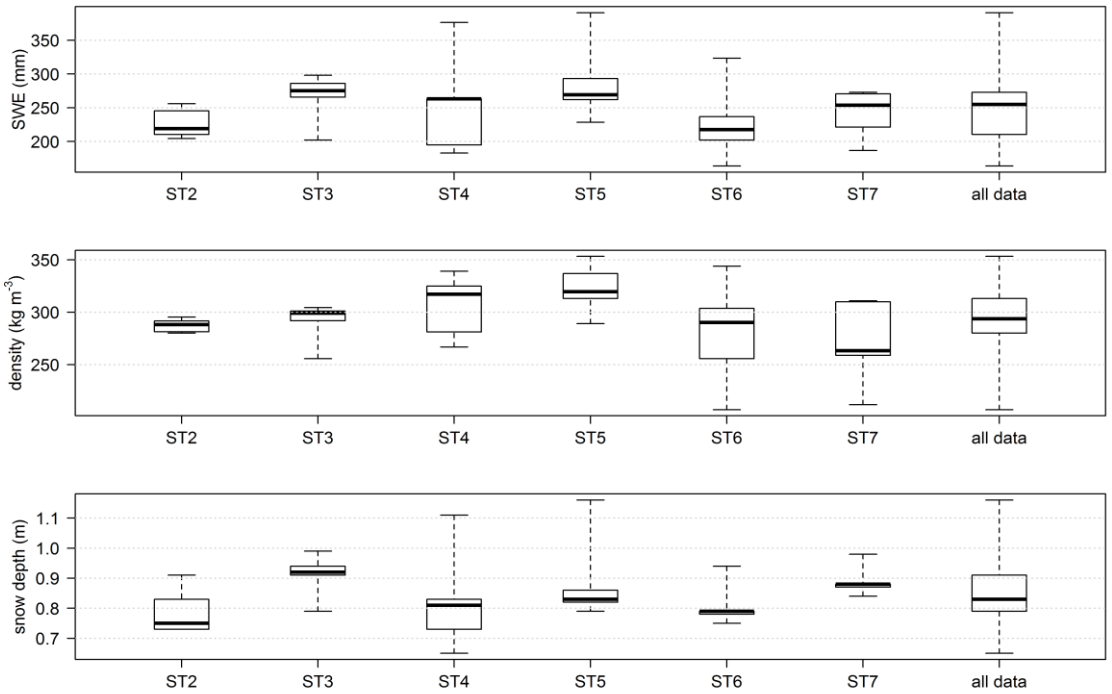

Figure 17. Variability of snow water equivalent, density and snow depth in each test plot and for all ST data.

Table 6. Average snow depth, density and SWE with coefficient of variations for each test plot.

Site	Environment type	Snow depth (m)	CV	Snow density (kg m^{-3})	CV	SWE (mm)	CV
ST2	spruce forest	0.79	0.10	287	0.02	227	0.10
ST3	tree line	0.91	0.08	290	0.07	265	0.14
ST4	open slope	0.83	0.21	306	0.10	256	0.30
ST5	next to bare fell	0.89	0.17	322	0.08	289	0.21
ST6	open mire	0.81	0.09	280	0.18	229	0.26
ST7	spruce forest	0.89	0.06	271	0.15	241	0.15
ALL	fell area	0.85	0.13	293	0.12	251	0.21

The Kendall correlations with p-values between all measured snow properties of all ST experiment points are shown in Figure 18. Figure 19 presents the correlation between mean snow properties of each test plot and topography details. Kendall correlation between mean snow measurement results and canopy closure determined from digital

photos is presented in Figure 20. Adjustment for ties is used when applicable in p-value calculations.

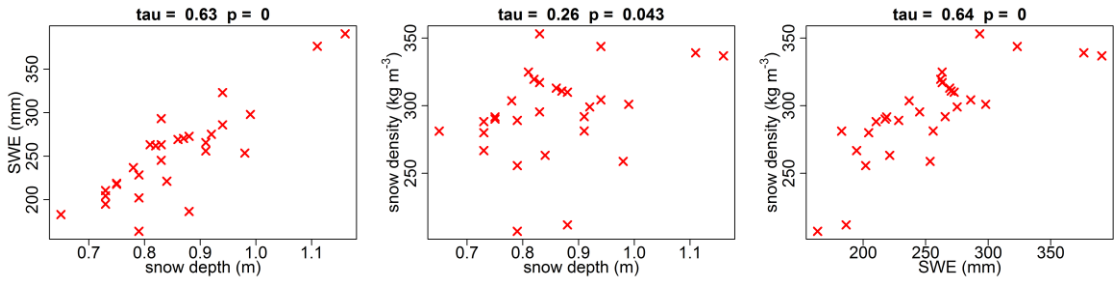

Figure 18. Kendall correlations between snow depth, density and snow water equivalent for all ST test sites. n = 30.

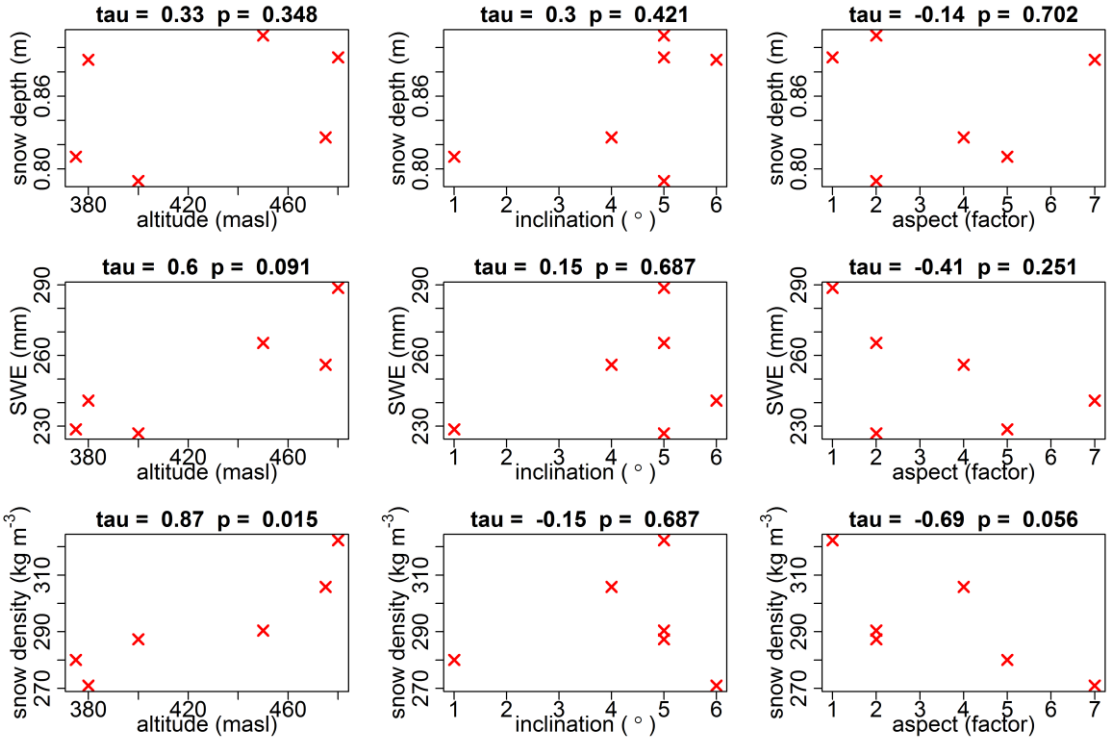

Figure 19. Kendall correlations (exact = false, because of ties) between topography and mean measured snow properties of each ST test plot. n = 6.

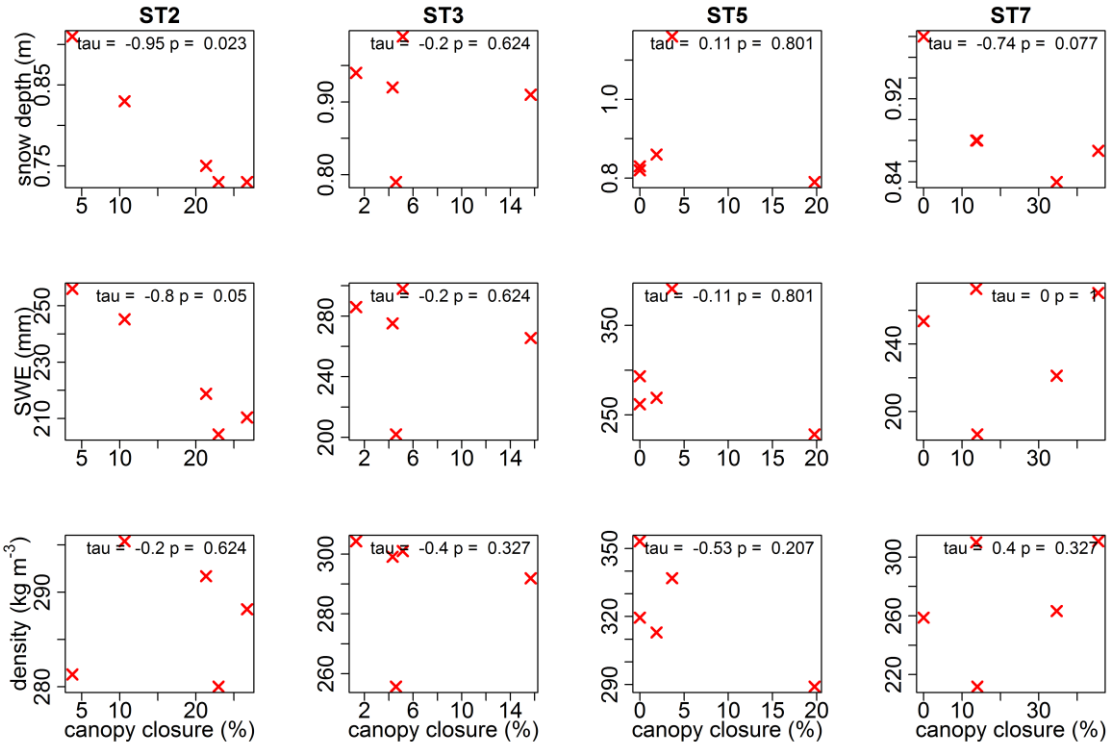

Figure 20. Kendall correlation between canopy cover and snow depth, snow water equivalent and snow density for test plots with trees. n = 5.

Kendall correlations and p-values between all plots with some canopy (ST2, ST3, ST5 and ST7 and snow properties are presented in Figure 21.

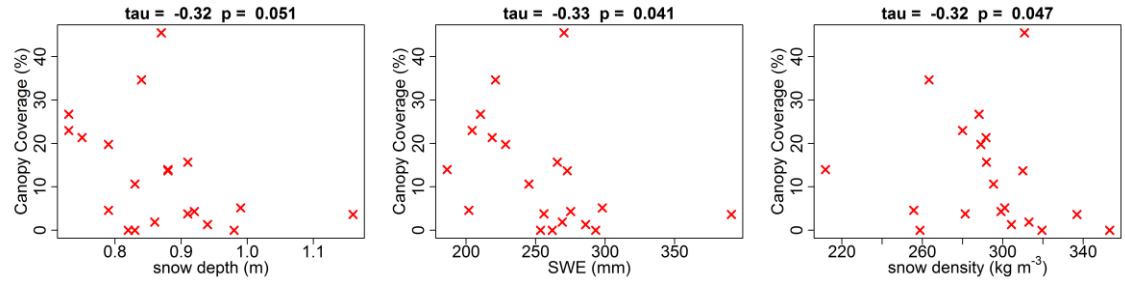

Figure 21. Kendall correlations with p-values between measured snow properties and canopy coverage at combined test plots with existing canopy coverage. n = 20.

5.3 Degree-day factors

Based on the dates for 30 cm and 0 cm of snowpack depth determined using the fluctuation of measured snowpack temperatures and measured air temperature the degree-day factors (Eq. 10) were calculated for each test point. The individual degree-day factors and mean and median values for each test plot are presented in Table 7. The mean DDF

for all data is 4.27 mm d^{-1} °C^{-1} and median 3.75 mm d^{-1} °C^{-1}. The calculated temperature degree factors for reference stations GC4 and GC7 are 1.93 and 2.47 mm d^{-1} °C^{-1}, respectively, for the last 30 cm of snowmelt.

To find out possible relations between determined degree-day factors and measured snow properties, topography and vegetation Kendall correlation was calculated for whole data set, median values for each test plot and separately for each test plot when applicable. The results are shown in Table 8.

Table 7. Determined temperature degree factors (mm d^{-1} °C^{-1}).

	ST2[1)]	**ST3**[2)]	**ST4**[2)]	**ST5**[2)]	**ST6**[1)]	**ST7**[1)]
1	3.66	3.75	2.84	6.95	2.64	2.56
2	4.81	NA	5.82	3.67	5.04	2.59
3	4.31	2.51	8.91	6.69	4.10	2.18
4	NA	3.75	2.38	4.59	NA	NA
5	5.32	NA	NA	2.97	3.05	7.43
Mean	4.53	3.34	4.98	4.97	3.71	3.69
Median	4.56	3.75	4.33	4.59	3.57	2.57

Snow density used in calculations: [1)] 329 kg m^{-3}, [2)] 349 kg m^{-3}

Table 8. Correlation between determined degree day factors and snow properties, topography and canopy closure.

	Snow depth	**Snow density**	**SWE**	**Altitude**	**Slope**	**Aspect**	**Canopy closure**
Tau (all)	0.14	**0.36**	**0.34**	NA	NA	NA	-0.06
p-value	0.33	**0.01**	**0.02**	NA	NA	NA	0.71
Tau (median plot)	-0.20	0.60	0.20	0.6	0	**-0.83**	0
p-value	0.72	0.14	0.72	0.14	1	**0.02**	1
Tau (ST2)	**0.91**	**1**	**1**	NA	NA	NA	-0.67
p-value	**0.07**	**0.08**	**0.08**	NA	NA	NA	0.33
Tau (ST3)	-0.82	-0.82	-0.82	NA	NA	NA	-0.82
p-value	0.22	0.22	0.22	NA	NA	NA	0.22
Tau (ST4)	**1**	0.67	**1**	NA	NA	NA	NA
p-value	**0.08**	0.33	**0.08**	NA	NA	NA	NA
Tau (ST5)	0.20	0.40	0.40	NA	NA	NA	-0.53
p-value	0.82	0.48	0.48	NA	NA	NA	0.21
Tau (ST6)	0.33	**1**	**1**	NA	NA	NA	NA
p-value	0.75	**0.08**	**0.08**	NA	NA	NA	NA
Tau (ST7)	0	0	-0.33	NA	NA	NA	-0.33
p-value	1	1	0.75	NA	NA	NA	0.75

5.4 Temperature-degree model

5.4.1 Critical moment for outflow

The model was first used to find out if the critical moment when the outflow from the snowpack begins can be determined. ST2.1 was used as the study location to compare the results with the adjacent GTK GC7 measurement station containing also gauge for soil water content at 20 cm below the ground. Model was calibrated to fit with the measured snow water equivalent on 17th of April and when the snow pack had completely melted at the test site. Degree day factor for the melt period was calculated as average between DDF determined with the temperature logger at ST2.1 and calibrated value for the accumulation season, because the DDF was defined for the last 30 cm of snow with the

temperature loggers. DDF is known to increase during the melt season being at its highest at the latter half of the melt because of the increased snow density and decreasing albedo. The calibrated parameters are presented in Table 9. Modeling results and reference measurements are depicted in Figure 22. The black vertical lines in Figure 22 mark the moment when the cold content of the snow pack is zero and liquid water holding capacity is full, e.g. the snowpack is ready to produce outflow. The vertical black line on the right in the lower graph in Figure 22 shows the time when the snowpack has completely depleted at GTK GC7 measurement station.

Table 9. Model parameters. (Kuusisto 1984, DeWalle and Rango 2011, Førland et al. 1996)

Parameter	**Value**	**Limits**
T_{crit}	1.1	-3.5 – 1.5
T_{melt}	0	-3 - 2
DDF[1)]	1.3	0.7 – 8
DDF[2)]	2.48	0.7 - 8
TSF	0.1	0.1 – 0.5
CCF	0.3	0.02 – 0.05
f	3	0 - 30
CF_s	0.86	1.05 – 1.8
CF_r	1	1.02 – 1.14

DDF: [1)] Until 15th of April, [2)] Since 16th of April

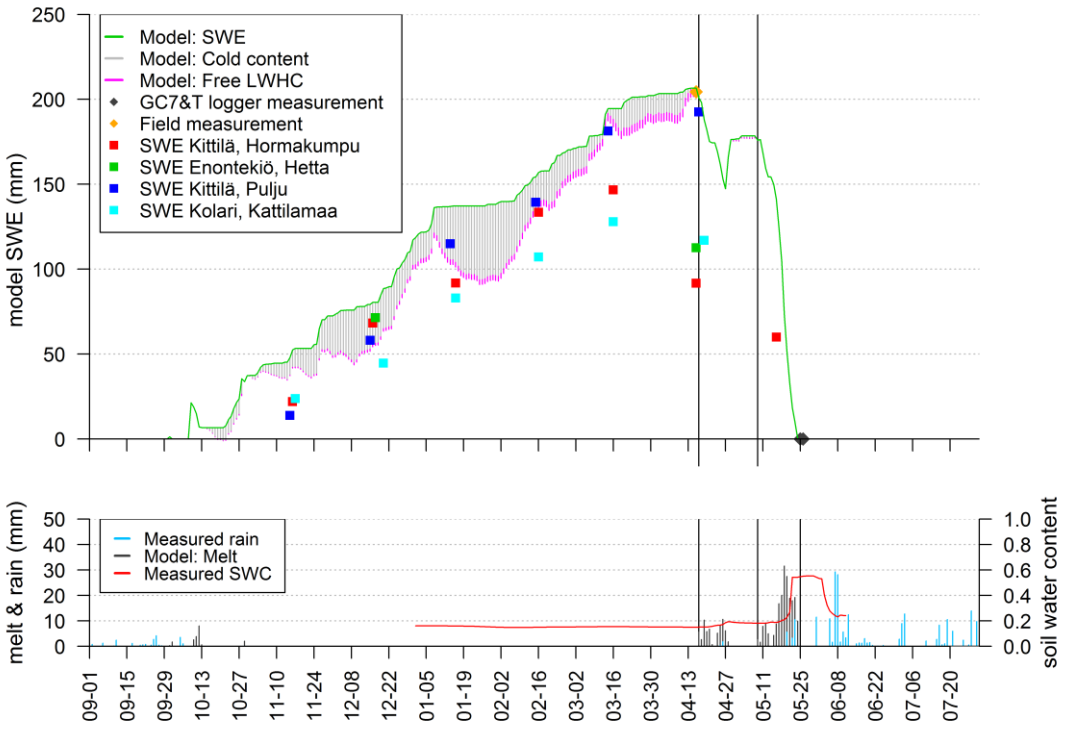

Figure 22. Upper picture: Modelled SWE, cold content and free liquid water storage capacity at ST2.1. Measured SWE at ST2.1 and four snow courses. Depletion date for snow cover at GTK GC7 reference site and at ST2.1. Lower picture: Modelled outflow from the snowpack as melt snow and rain at ST2.1. Soil water content measured 20 cm below ground at GTK GC7. Vertical black lines show the time when snowpack is isothermal 0 °C and LWHC is full, except in the lower graph the rightmost line marks the date when GTK GC7 is out of snow.

5.4.2 Spatial variability

Next the model and determined degree day factors were employed to explore the spatial variability of the snow accumulation and melt. Precipitation measurement data from single measurement point as input to the model used in this study is not capable to reproduce the large spatial variation of the snow water equivalent with single correction factor for snow precipitation CF_s without additional parameters. Therefore a simplified approach was employed. The correction factor for snow precipitation is set to include also effects of topography, vegetation and snow redistribution in each measurement point.

Linearity between SWE and correction factor for solid precipitation was assumed (Eq. 12). A linear equation (23) was determined to maximize the goodness of fit R^2 between the model and the measured SWE's on 16 - 17th of April. The equation was derived using the minimum and maximum values of the measured SWE and calibrating the correction

factor for solid precipitation so that the modelled and measured SWE values matched with each other. Finally a line was determined between the two points.

$$CF_{s\_x} = 0.0036 \times SWE_{meas\_x} + 0.12 \quad (23)$$

where CF_{s_x} is the correction factor for solid precipitation at study point x
SWE_{meas_x} is the measured SWE at study point x
x is the study point [ST2.1….ST7.5].

Calculated with equation 23 the lowest value of correction factor for snow precipitation was 0.71 and highest value 1.53 for the dataset used in this study. The lowest value equals to measured SWE of 163.6 mm at ST6.4 and highest value to 390.8 mm at ST5.3.

The temperature degree factor was assumed to be constant during the accumulation period as the main interest of this study is in the snow melt. The degree-day factor is found to be increased during the spring (e.g. Kuusisto 1984, p. 92; DeWalle et al. 2002), thus a linear increase between 16th of April to 8th of June is applied (Figure 23). The approach was adapted from a study by Federer and Lash (1983) cited by DeWalle and Rango (2011, p. 277). The equation for DDF is

$$DDF_{day} = \begin{cases} DDF_a, & date < 16.4. \\ DDF_a + \frac{1}{8} \times (DDF_m - DDF_a) \; to \; DDF_m, & 16.4. \leq date \leq 8.6. \\ DDF_m, & date > 8.6. \end{cases} \quad (24)$$

where DDF_{day} is the DDF applied for a day
DDF_a is the DDF set for the accumulation season
DDF_m is the DDF determined using temperature loggers.

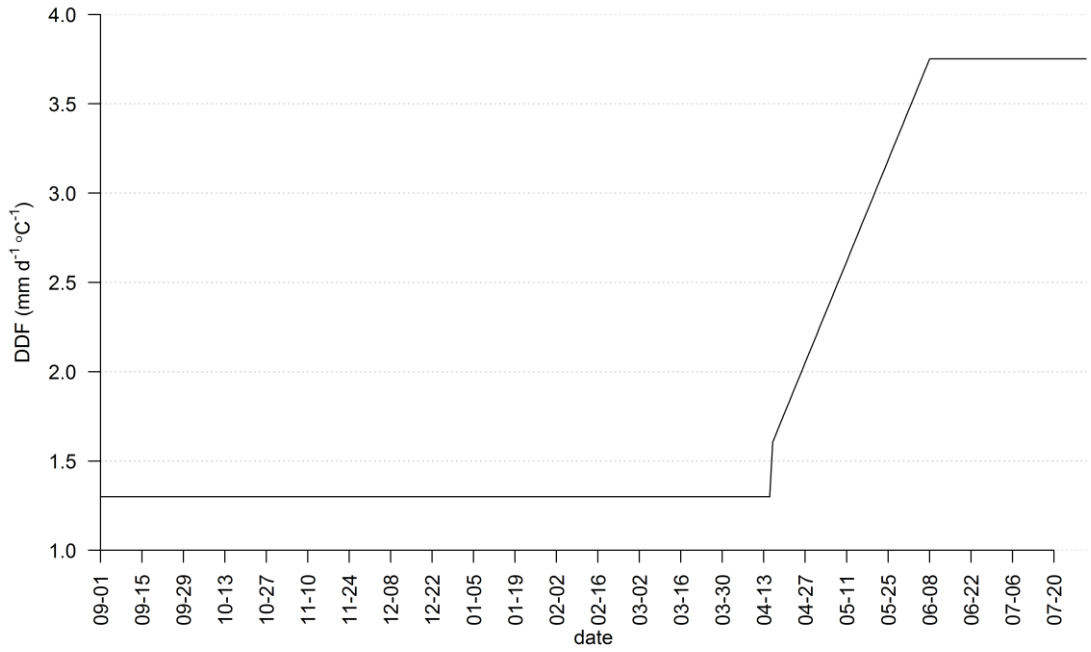

Figure 23. Shape of DDF applied in model.

Figure 24 presents the modelling results for all test points in the study area as well as the spread of SWE inside each test plot and overall experiment area. Spread of the dates for all snow melt in each test point is included. The measurements of the closest snow courses are also included in Figure 24. The RMSE is calculated to be 3.74 and $R^2 = 0.996$. The error in days for each test point between the model and measured date for the complete snow melt and basic descriptive statistical parameters are shown in Table 10. The model was run also by using overall median DDF and plot specific median DDF's. The results are presented as tabulated values in Annex 2.

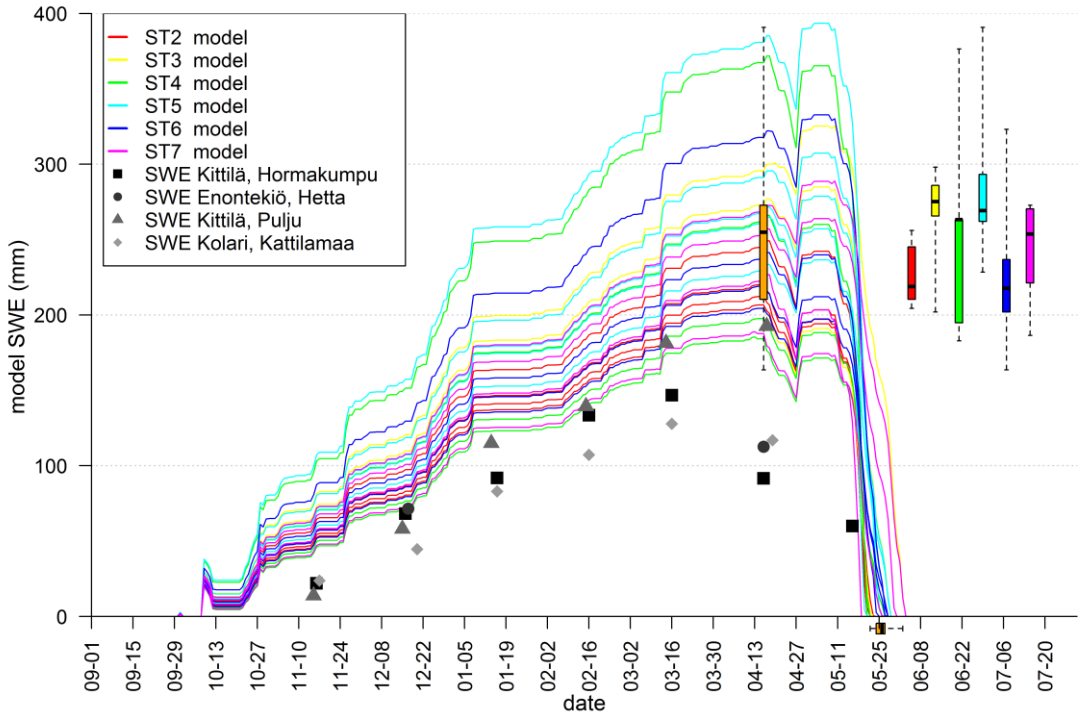

Figure 24. Modelled SWE for each test point. Boxplots of measured SWE data for each experiment plot at the right side of the figure. Boxplots for combined ST SWE field measurement data in orange as well as dates for complete snow cover depletion determined by temperature loggers.

Table 10. Difference between modelled and measured day for complete snow melt in days. Overall mean and median: -0.29 & -1 days. Overall SD and IQR: 3.8 & 6 days. RMSE = 3.74.

	ST2	**ST3**	**ST4**	**ST5**	**ST6**	**ST7**
1	-2	-1	4	-5	1	-5
2	-2	NA	-2	4	1	-2
3	-5	4	-5	-1	-1	3
4	NA	5	5	2	NA	NA
5	-5	NA	NA	5	2	-7
Mean / SD	-3.5 / 1.73	2.66 / 3.21	0.5 /4.80	1 / 4.06	0.75 / 1.26	-2.75 / 4.35
Median / IQR	-3.5 / 3	4 / 3	1 / 7	2 / 5	1 / 0.75	-3.5 / 4.75

For comparison the model was ran using degree-day-factors calculated with equations 11 and 12 by Kuusisto (1984). Because the density was measured in the beginning of the melt season, a correction factor of 0.7 was added for the degree day factor on the 8th of

June. Otherwise a similar linear approach for DDF was used as in the temperature logger model. The results are shown in Figure 25 and Table 11. The goodness of the fit R^2 is 0.996 for modelled SWE on 16th of April and RMSE for the snow melt completion date is 2.11. Comparison of the spread of the modelled error between temperature logger model and Kuusisto model in days is shown in Figure 26.

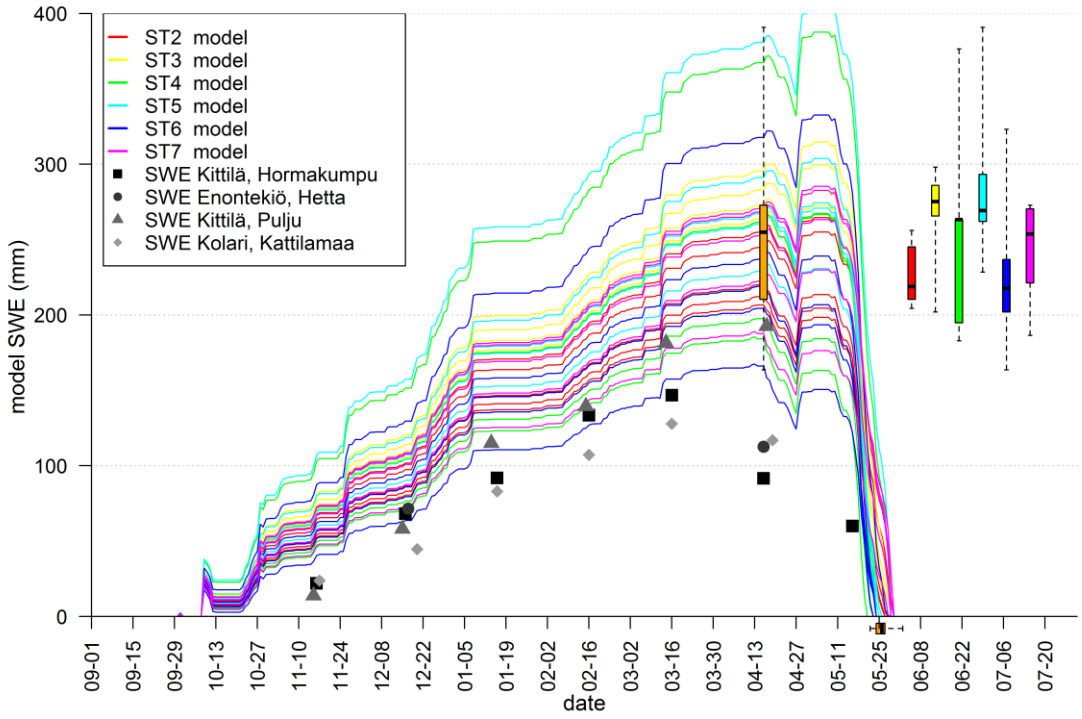

Figure 25. Modelled SWE for each test point. Boxplots of measured SWE data for each experiment plot. Boxplots for combined ST SWE field measurement data in orange as well as dates for complete snow cover depletion determined by temperature loggers. Kuusisto density based (forest & open) equations for DDF used.

Table 11. Optimized Kuusisto (1984, p. 97) density equations. No logger data, only density measurements on 16/17th of April. Mean/median: 0.25 & 0 days, SD/IQR: 2.14 & 2 days. RMSE = 2.11.

	ST2[2)]	**ST3**[1)]	**ST4**[1)]	**ST5**[1)]	**ST6**[1)]	**ST7**[2)]
1	1	0	1	-1	-3	-3
2	5	NA	1	1	1	-3
3	0	-1	3	3	-2	-1
4	1	4	-1	-1	-1	0
5	2	NA	1	0	-3	3
Mean / SD	1.8 / 1.92	1 / 2.65	1 / 1.41	0.4 / 1.67	-1.6 / 1.67	-0.8 / 2.49
Median / IQR	1 / 1	0 / 2.5	1 / 0	0 / 2	-2 / 2	-1 / 3

[1)] Equation 11 for open used. [2)] Equation 12 for forest used.

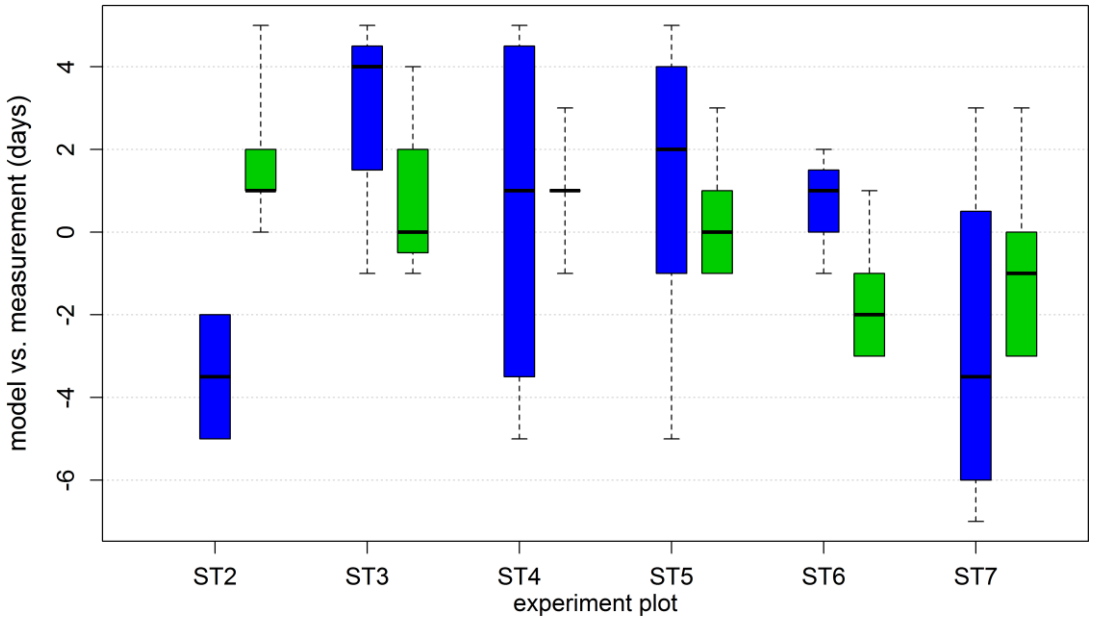

Figure 26. Spread of model vs measured error in days for snow melt completed. DDF's determined using temperature loggers (blue) and Kuusisto density equations (green).

6 DISCUSSION

6.1 Temperature logger data interpretation

Diurnal standard deviation (Reusser and Zehe 2011) of smoothed temperature data was found to be the most useful method to determine the day when the temperature logger is free of snow. In determining the timing when the temperature logger was free of snow (Figure 11) it was noticed that the temperature is first rising slowly towards the air temperature. This is interpreted to be caused by the decreasing insulation depleting snowpack above the sensor and/or shortwave radiation penetrating through the snow (Pomeroy and Brun 2001; Gray 1981). In Figure 15 the same phenomena can be seen as small rise in standard deviation of the logger temperatures. At approximately 12:00 during the midday a sharp peak can be seen in the logger temperatures (Figure 10). This is expected to be caused by the short wave radiation penetrating through the snow and absorbed by the temperature sensor. The peak can be seen at the same time also after the logger is estimated to be free of snow, which strengthen the assumption of heat absorption of solar radiation. This phenomena increases the daily standard deviation of the sensor temperature and is estimated to cause maximum error of one day in the determination of the date of freed snowpack sensor. Therefore the observed peaks were removed from the further analysis.

Daily standard deviation of 2.0 °C was used as the threshold to determine the date when the logger is revealed from snow. In this study threshold values between 0.9 - 2.3 °C were found to be usable in sensitivity analysis. Accuracy of the temperature sensor, insulating properties of the snowpack and the magnitude of fluctuation of air temperature increase the uncertainty below the lower limit. Upper threshold limit is derived also by the accuracy of the temperature sensor but mainly from the fluctuation of the air temperature. Below and above the limits the sensitivity of the method increases and change of 0.1 °C in threshold value increases or decreases the logger reveal date often one day or more. Within the determined limits the change of 0.1 °C in threshold temperature has usually no impact on logger reveal date and maximum change of one day is observed rarely.

6.2 Variability of snowmelt timing

The spread of the complete snow cover depletion in the experiment area is found to be 11 days and 12 days on 30 cm snowpack height. Earliest measured date when all snow was melt is 22nd of May while the latest is 2nd of June 2014. The snow in the test area melted later than the average ending date of permanent snow cover in the region during 1981 – 2010 (FMI 2015), which is again seen as the result of higher elevations of the study area compared to the surrounding region.

It can be seen from Figure 16 that spread is higher in forested areas (ST2, ST3 and ST7) whereas the smallest spread can be found from an open mire (ST6). The forest plot ST7 at northeastern slope is observed to have the latest melt dates, which is assumed to be a result of the reduced amount of solar radiation and highest canopy coverage of the test sites. The test plots at highest elevations (ST4, ST5) towards southwest are observed to have earliest melt dates. The agreement between GTK reference measurement sites GC7/GC4 and test plot ST2/ST3 is found to be reasonable good. The difference of one day between ST2/GC7 at 30 cm snowpack height can be explained by the natural variation but it is possible to be caused also by the uncertainties of the measurements.

Despite the uncertainties in the temperature logger data interpretation, the method reveals the mesoscale variation between the plots and microscale variation within the plots of snowmelt (Figure 16).

6.3 Snow pack properties

6.3.1 General snow conditions at study winter

It can be seen from the field measurements on 16 - 17th of April 2014 that the average snow water equivalent at the fell area (251 mm) is above the average maximum SWE in the region during the period of 1971 – 2000 (Veijalainen et al. 2012). On the other hand the maximum SWE at the nearest SYKE snow courses (193 mm at Kittilä, Pulju on 17th of April 2014, with remarkably lower values at the three other SYKE snow courses in the region) was lower than the maximum average SWE during the period of 1971 – 2000.

Mean snow pack depth measured on the area was 0.85 m. According to Kuusisto (1984) the mean maximum snow depth in northern Finland has been between 50 and 80 cm

whereas the average snow depth on 31.3 during period of 1981 – 2010 in the studied region was 60 – 80 cm (FMI 2015).

The measured precipitation (377.9 mm) at FMI Kenttärova site during the study winter was higher than during the period of 1981 – 2010 in the region (320 - 350 mm), especially during winter and spring seasons.

These observations indicate the average amount of snow in the region during study winter of 2014 was generally below the long term average but at the fell area under study the amount of snow was higher. This is expected to be a result of the topography and specifically the elevation of the area. However, the precipitation measurements indicate that even there were more precipitation during the study winter than longer term average there was less snow in the region. On the other hand the precipitation measurements at Kenttärova site, which was adjacent to the experiment area can explain the higher amount of snow in study area.

The measured average snow density at the area during 16 - 17th of April 2014 was as high as 292.8 kg m^{-3} which is probably a result of the snow pack compression metamorphosis due to relatively high SWE on the fell area (Kuusisto 1984, p. 43). Other explanation is that the measurements were found out to be done close to the onset of the melt period, thus melt metamorphosis is also expected to be already ongoing at the time of measurements.

6.3.2 Variability of the snow properties

Snow water equivalent

The highest average snow water equivalents (Table 4) in the study area were measured at the edges of the open areas where the increasing forest cover is expected to act as a trap for the wind redistributed snow (DeWalle and Rango 2011, p. 32). Spruce forest plots with highest canopy density as well as open mire were found to have the lowest average snow water equivalents. The low SWE at the forest sites is assumed to be caused by the snow interception and evaporation at the forest canopy (Dingman 2008, p. 181), which also restricts the redistribution of snow to the area. The result in open mire was unexpected as the open areas typically attract more snow than the forests. A statistically significant negative correlation of was found between the canopy coverage and SWE at

forested plots (Figure 21), which was expected. SWE was also found to have a high correlation (0.64, 0.63, p = 0) with the snow density and depth (Figure 19) which is obvious as the SWE is derived directly from both of the quantities.

The coefficient of variation for SWE (Table 6) was found to be highest at open southwestern slope (ST4) at the elevation of 475 masl. The second highest CV was found at the open mire at 375 masl. The high variability at ST4 is partly explained by one test point where a small water stream was observed and the SWE was exceptionally high (376.4 mm). Lowest coefficient of variation of SWE was found at the forested spots at ST2, ST3 and ST7 at elevations of 400, 450 and 380 masl, respectively. The variability of the SWE is found to be lower in forested areas than open in this study.

Snow density

The snow density was found to have a positive correlation (Figure 19) with the altitude. Highest value accounted to 322 kg m^{-3} at ST5 with elevation of 480 masl and lowest value 271 kg m^{-3} at ST7 at the elevation of 380 masl. The result is expected to be a consequence of combined altitude and change in vegetation. The less dense vegetation in higher altitudes permits increased wind speeds which are known to increase the density of the accumulated snow (Rasmus 2005). The hypothesis is supported by the negative correlation (Figure 21) found between the plots with some forest and snow density. Negative correlation was also found between snow density and aspect factor (Figure 19), which can partly be explained also by the altitude as the highest experiment points are located on the western-southern side of the slope. Other explanation can be the larger exposure for the solar radiation on the southern slopes, which can increase the densification of the snowpack.

Open mire (ST6) at 375 masl accounts for the highest CV of snow density (Table 6) whereas the second highest variation is found at the spruce forest (ST7) at 380 masl at the northeast slope. Lowest variability's were found at the southwestern plots with forest at ST2 and ST3. The variability of snow density was observed to be generally lower at the southwestern slopes. No clear dependency was found with other topography or vegetation parameters. The smaller variability at the southeastern slope could be a result of faster progress in snowpack metamorphosis due to exposure to solar radiation.

Snow depth

The average snow depth (Table 6) was found to be highest at ST3 at tree line, ST5 close to the bare fell and ST7 at spruce forest on northeastern slope. The first two are explained by the trapping properties of redistributed and blowing snow. The last can be explained with delayed melt metamorphosis of snowpack due to reduced solar radiation caused by the topography and forest. This is supported by the lowest measured average snow density at ST7. Highest variability of snow depths is found at open spots at elevations of 450 and 480 masl excluding the open mire at 375 masl whereas lowest variability was generally observed in forested plots.

Low amount of data points at each test plot introduces uncertainty in the results as it can be questioned if the selected test points represented typical properties of the area. Also statistical analysis typically need more data points, thus the variability analysis can be expected to be a rough estimation. However, the overall number of data points was sufficient (Figure 18). There can be also smaller error in field measurement results done using the snow cores.

The determination of canopy coverage using digital photography is also a rough estimate. There were deciduous trees with leaves already present at the time when the pictures were taken and the reduction of canopy coverage (%) for these cases is done by visual estimation. Another uncertainty comes from the accuracy of setting the camera directly towards the zenith – a spirit level was used. Third point in accuracy is the limited angle of view of the camera – only upper parts of the canopy was often captured on the pictures. Still when compared to the canopy density material provided by Metla (2013) the average measured canopy densities are within the same magnitude (data not shown in this study).

6.4 Degree-day factors

The determined degree-day factors (Table 7) show large variability, which is expected already from the variability of the measurement results of the snow properties, topography, vegetation and accuracy in determination of the snow melt dates. The DDF values are within the range found in literature (e.g. Kuusisto 1984, DeWalle and Rango 2011). Positive and statistically significant correlation was found between snow density measured on 16 - 17th of April and degree day factors determined for each test plot (Table

8). This observation agrees with the theory as the degree-day factor increases with the density because of the increased thermal conductivity of the snow. Negative and statistically significant correlation between aspect class and median DDF of each test plot (Table 8) can also be explained by theory because southern slopes receive more solar radiation which increases the melt rate. No statistically significant correlation was found between the determined canopy coverage and degree day factor, even though a correlation was expected. Anomalously high DDF-values were found at ST4.3 and ST7.5. The first is probably caused by a meltwater stream assumed to increase the melt rate and observed at the location during the fetching of the loggers. At the second point the high value could be explained by a hummock and snapped dead trees next to the loggers, which can lead to additional absorption of shortwave radiation, thus accelerating the melt.

The biggest discrepancy compared to theory is found between test plots ST2 and ST3. ST2 is at lower elevation with larger canopy coverage than ST3. Still the mean and median DDFs are found to be larger in ST2. However, the same behavior is found using data from GTK reference stations. The explanation can be natural variability as the differences between altitude and canopy coverage is not large. Measurements by Kuusisto (1984, p. 94) also show that the variation of the DDF can be stochastic at lower canopy densities even though an overall decreasing trend of DDF can be seen with increased canopy density.

Compared to degree-day-factors determined for the last 30 cm of snow using the measurement data from GTK reference stations, the values calculated with the temperature logger data are clearly higher. The differences can be explained by the solar radiation absorbed by the temperature sensors and the resulting increased melt speed at the logger locations, especially at the southern slopes and open areas. Other explanations include the assumption that the snowpack height is 30 cm after the upper sensor is free of snow. There is uncertainty caused by the dimensions of the sensor. The temperature logger was attached to the wooden stick in a position where the middle point of the logger was at 30 cm above the ground. The vertical height of the logger in its installation position is 33 mm, which gives the lower and upper level of the logger a heights of 28.35 and 31.65 cm, respectively. It can be assumed that there is only 28.35 cm of snow below the sensor. It was also noticed when fetching the loggers from the field that some of the loggers where slightly pushed downward on the wooden stick and some of the sticks were sank to the ground approximately 1 cm. The total possible displacement was not measured

in situ and is estimated to be max 2.5 cm. The reason for this possible downward movement is expected to be the metamorphosis and densification of the snowpack which can push the loggers towards the ground. For the logger on the ground level (0 cm) the actual snowpack height can be +23 mm, which is the height of the temperature logger installed to the ground. By combining the observations above, the actual snowpack height between the sensors can be as low 23.55 cm instead of 30 cm. The possible error of the snow pack depth estimation can lead to too high calculated degree day factors.

Finally, natural variation of snow density is causing error as the density used in the calculation was constant for each test plot. The snow cover was also disturbed during the installation of the loggers, which increased the snow density at the test points. The density of the test plots was not known for the time period which was used in degree day determination.

6.5 Snow model

6.5.1 Critical moment for outflow

It can be seen from Figure 22 that the fit between the snow water equivalent determined by the model and the onsite measurements is very good. The difference between modelled and measured SWE on 16th of April is 2.2 mm and the difference between model and measured snow cover melt is one day. In turn there is a minor gap compared to the snow course measurements even between the best fit snow course data from Kittilä - Pulju and the model, especially at the first half of the accumulation season. The most probable explanations include large natural spatial variation of the snow cover and the topographic difference of the test area and the snow courses. Other explanations can be the constant threshold limit determining the precipitation type in the model as well as the correction factor applied to snow precipitation. According to Kuusisto (1984, p. 28) the threshold temperature for equal probability for snow and rain precipitation increases during the winter which can lead to increased share of snow precipitation during the spring period compared to autumn. The conclusion is that the snow course measurements are not representing well the snow conditions at the experiment area, which can be a result of differences in terrain type and topography, especially altitude, explained earlier in this chapter. Also the distance between the snow courses and study area causes differences in snow conditions.

The modelled cold content and water holding capacity (Figure 22) are increasing during the winter, former reaching its maximum values during the coldest period of time in January and the latter when the snow water equivalent of the snowpack reaches its maximum on April. The model shows that the cold content of the snowpack is satisfied on 16th of April (below 1 mm already on 14th of April) and the LWHC is satisfied first time on 17th of April initiating outflow from the snowpack. The timing of the field measurements on 16 - 17th of April were excellent as the maximum SWE is assumed to be captured, just when the first outflow period starts. The soil water 20 cm below ground at GC7 increases slightly on 21st of April supporting the observations from the model

After a short frosty spell the main melt period is modelled to start on 9th of May. First the melt is relative low and there is even one cold day when no melt occurs on 14th of May. After that the final melt phase begins on 15th of May and the SWC at 20 cm below ground at GC7 starts to increase on 18th of May reaching its maximum value on 22nd of May, three days before all snow has melted from the point. The SWC value close to maximum is held for 5 days after all snow is melted at the test point.

A 3 - 4 days gap is found between the start of the model outflow and increase in soil water content 20 cm below the ground. It can be explained by the shortcomings in the model; inadequate liquid water routing through the snowpack, the assumption of homogenous snowpack, unavailable calibration data for the cold content and constant maximum liquid water holding capacity-%. Additionally the modelled liquid water is not expected to drain from the snowpack after the melt/rain ceases. Also the water percolating through the soil to depth of 20 cm has some lag, which explains the gap. Finally, end of the permanent snow cover date was measured to be one day later at ST2.1 than GC7 which can be explained by the microscale variation of the snowmelt.

The temperature data from the loggers on the ground and 30 cm above the ground alone is not found sufficient to estimate the time when the snowpack is ready for outflow. Calibration measurement data of at least SWE is needed. Probably, if there were more temperature loggers placed vertically to snowpack higher than 30 cm from the ground, it could be possible to estimate when the snowpack is ripe, because the temperature profile of the snow cover could be determined in more detail. Thus, also the critical point for outflow from the snow pack could be estimated without additional field measurements.

6.5.2 Spatial variability

The wide spread of the SWE in the study area and the relative abundance of snow compared to the surrounding snow courses can be seen in Figure 24. The combination of several environment variables in correction factor for snow precipitation gives a good starting point of SWE to the melt season in the model. The goodness of fit between the model and measured SWE's on 16 - 17th of April is 0.996, which is considered excellent. Normally the correction factor for snow precipitation is larger than 1 but now a wide spread of factors from 0.71 to 1.53 was used. The values below 1 are a result of environmental variables included in the correction factor for solid precipitation. The high natural variation of snow accumulation tolerates the large spread. In a study by Gray et al. (1979) ridges and hilltops accumulated 50% of SWE whereas steep hills and valley slopes 285% of snow compared to 100% on fallow level plains (Pomeroy and Brun 2001, p. 62). However, the approach can lead to big errors in SWE of accumulated new snow as it does not separate for example the topography and vegetation details and wind redistribution and the actual snow precipitation.

It can be observed from the Figure 24 that the vast majority of the modelled dates for end of the snow melt season hits the spread of the measured dates the median error being -1 days with RMSE of 3.74 days. It can be seen from Table 10 that in average the modelled snow melt is 3 - 4 days early compared to measurements at the forest sites except at the forest line where the average melt is slower (3 days late) in model than measured. The difference is smallest in open sites with one day or less delay in the mean model melt versus measured. In additional analysis it was found out that the Kendall correlation between the difference of model vs. measured and the determined degree day factors was -0.43 ($p = 0.004$, $n = 24$), which signals to systematic uncertainty in DDF determination. Large DDF's tend to result to too fast modelled melt and small DDF's to too slow.

The mean modelled snow melt date was early compared to measured dates at forest site ST7. It can be explained by the slope aspect of northeast, which leads to later reach of the sun beam to the site. Figure 16 also partly explains the situation, the snow at ST7 is melting later than in the other sites. The model could be improved by implementing a correction factor for the forested test plots at the northern slopes.

At forest site ST3 the modelled snow melt was also early compared to the measured dates but the reasons are expected to be different than at ST7. Some of the test points are

probably exposed to more sunlight which leads to increased heat absorbed by the temperature loggers, thus increased melt rate disturbing the melt rate determination. Also the density used in DDF determination is assumed to be constant which is not expected to be reality and this increases also uncertainty in the results.

The standard deviation and IQR of the modelled versus measured date for snow melt complete was smallest at open mire (ST6) and largest at open southeast slope (ST4). The smallest spread on the open mire is assumed to be a result of open, flat and relatively homogenous terrain type, which is expected to be least vulnerable for the errors caused by differences in absorbed solar radiation of the temperature loggers.

Model was also run using median overall DDF determined using the temperature loggers, with slightly increased error (RMSE 3.81 days, Annex 2). Using median determined DDF of each test plot clearly improved the results (RMSE 3.19 days, Annex 2). The error was increased at the ST6 (open mire) and decreased at other test plots.

Finally, the model was ran using the measured densities at 16 - 17th of April and the DDF's determined based on the Kuusisto density based empirical equations. The results are presented in Figure 25 and Table 11. The RMSE of 2.11 days was approximately one day smaller compared to the best model using DDF's determined with the temperature loggers. The change was biggest at ST4 (open southwest slope) and at the forest site (ST7) on northeastern slope. The discrepancy between ST2 & ST3 was not visible. At the open mire the DDF's determined by temperature loggers gave better results than the Kuusisto equation for open area. Comparison of the spread modelled using Kuusisto equations and individual temperature logger DDF's is presented in Figure 26. The degree day factors determined using empirical Kuusisto equations based on snow density are not affected by the solar radiation and other uncertainties in method using temperature loggers. The density of the snow correlates with the age of snow (albedo, compaction) and the liquid water content (Kuusisto 1984, p. 97). The snowpack was not disturbed when the densities were measured whereas the density of the snowpack was increased when the temperature loggers were installed. The measured densities were also in the range of 200 – 400 kg m^{-3}, where the Kuusisto equations are applicable. Additionally the equations are based on larger sample size and cover time series analysis instead of single winter as used in this study (Kuusisto 1984). Thus, the measurement of snow density at the time of maximum

SWE would be economically more efficient for snow melt modelling but lacks the possibility of acquiring real time data of the snow pack.

The conclusion is that melt rates determined by the low cost temperature loggers and the implemented model are most accurate in open and relatively homogenous terrain type in microscale level. On mesoscale level with more complex terrain type and forest, median determined melt rates are recommended to be used. With temperature loggers installed on the ground and 30 cm above the ground field measurements of the snow pack properties are suggested to be executed at least once, preferably close to the time of maximum snow water equivalent to calibrate the model. If additional temperature loggers are installed above the 30 cm from the ground the need for other measurements of snowpack properties can probably be eliminated. The biggest individual source of uncertainty is assumed to be the natural variability of direct solar radiation reaching the temperature loggers and lack of more detailed information of the change in snow pack structure and properties during the snowmelt.

6.6 Recommendations for future work

There are many advantages and disadvantages in the method. Some of them are listed below followed by the main sources of uncertainty and ideas for improvement.

The pros of the method:

- cost efficient
- continuous measurements
- spatial coverage
- accuracy in simple terrain type

The cons of the method:

- less accurate in complex terrain types
- requires manual work
- covering big areas is resource intensive
- uncertainty caused by solar radiation

Main sources of uncertainty:

- Solar radiation absorbed by the sensors resulting to too high temperature readings and melting of the snow adjacent to the logger
- Displacement of the upper logger due to compression of the snow
- Unknown physical snow properties during the end of the melt period
- Inaccuracy in the method how the date when logger is free of snow determined
- Disturbance of the snowpack during the logger installation
- Natural variability of the terrain type and vegetation resulting to abnormal melt rates, which are not generally representative in the measurement area and difficult to model

The impact of direct solar radiation to the loggers on the ground could be prevented by installing the loggers slightly underground as in study by Lundquist and Lott (2008). The loggers above the ground in the snow pack could be painted in white or smaller size logger could be used to minimize the absorbed solar radiation. The installation procedure could be improved by digging a smaller pit to the snow and careful handling of the excavated snow during the process to minimize the disturbance of the snow pack. For best result the loggers should be installed before the snow season. This way also the test points could be selected so that small water streams, hummocks and undergrowth, which cannot be detected below snowpack, would not disturb the measurements and the placing of the loggers would represent more accurately the area under interest. The possible displacement of the upper logger due to snow metamorphosis could be prevented be installing a small plate on the ground, below the stick which is used to hold the logger.

The snowpack properties during the melt could be estimated in more detail using physical snow models including the modelling of the snowpack structure, which can increase the accuracy of the determination of the melt rates. The downside of such models is the increased need for input measurements, such as short and long wave radiation and humidity. Also the preferred frequency below one day for the input measurements is recommended. More research could also be done to develop the method how the date when the loggers are free of snow is determined. For example the impact of solar radiation to the temperature fluctuations could be studied in more detail. Using wireless connections the loggers could be utilized also to receive real-time information of the snow pack for operational use.

7 SUMMARY

At high latitudes the melt of the snowpack has a significant impact on the hydrology being usually the largest individual event during the hydrologic year. The snow distribution and processes are known to have a high variability and the measurements of snowpack are resource intensive. Therefore there is a need for simple and cost efficient methods to catch the spatial and temporal variation of snow melt to predict its impact to ground water levels, river discharges and floods.

In this study the snow melt processes and rates were studied in a Pallas subarctic fell area using low cost temperature loggers, statistical analysis and an empirical snow model. Six test plots with different topography, vegetation and terrain type were used for the study. Adjacent acoustic snow measurement stations (GTK) were used to validate the results.

Snowpack temperatures on the ground and at a constant height of 30 cm at the test plots were recorded using low cost temperature loggers between 19th of April and 15th of June 2014. The fluctuation of the logger temperatures were used to study the spatial variability of the snow melt processes and rates. Based on the measurement results degree-day-factors were determined and utilized in a snow model to find the critical moment for outflow from the snowpack and to validate the results. Climate data from FMI was used as the input for the snow model.

The spatial and temporal variability of the end of permanent snow cover was captured with the method with reasonable good agreement of the melt timing with the GTK reference measurement stations. Forested areas were found to have higher temporal variability than open spots in snow melt. Open mire accounted for smallest spread of two days in depletion of the permanent snow cover.

The snowpack depth, density and snow water equivalent were measured during 16 - 17th of April 2014 at the time when the snow water equivalent was at its highest point to obtain information of the snow cover properties in the area and for model calibration. The properties of the snowpack were analyzed and compared to the SYKE snow course measurements in the region. It was found out that the amount of snow in the regional level during the experiment winter was lower than longer term average. Nevertheless there was more snow at the fell area under study than long term average in the region.

Average values of degree-day factors determined with temperature loggers were found to be higher than the ones determined using GTK data from the adjacent stations. Biggest contribution was identified be the solar radiation absorbed by the temperature loggers. Other source of error was the uncertainty in distance between the logger on the ground and at 30 cm height from the ground. Finally natural variation in snow density adds error to the results as the actual density in the final melt phase was not known. Physical snow model could be used in future studies to improve the knowledge of physical state of the snow during snowmelt, thus reduce the uncertainty in melt rate determination.

The critical moment for outflow determined using empirical snow model was found to be reasonably good. The difference between the time when the snow pack was ripe, i.e. ready to produce outflow determined by the model and time when increase in soil water content was measured was 3 - 4 days. The gap was explained by the natural microscale variation in snowmelt, shortcomings in the model such as lack of transmission of the liquid water and the delay of the liquid water reaching the moisture content sensor at 20 cm below the ground.

Snow melt rates determined by the temperature loggers were finally validated with the empirical snow model. The biggest impact for uncertainty was found to be natural variation of solar radiation, which disturbed the measurements the absorption of solar radiation by the loggers, thus increasing melt speed. Other significant cause of uncertainty was assumed to be the unknown natural variability of the snow density during the melt period. However, reasonably good agreement with RMSE of 3.74 days between the model and measured dates for the end of permanent snow cover in microscale level was found. In mesoscale level the RMSE was improved to 3.19 days, however, the accuracy decreased at open mire.

The method was found to be most accurate in open mire with flat and relatively homogenous terrain conditions. In more complex topography and spots with forest cover median determined melt rate values are recommended to be used. The method is found to be a cost effective and reasonable accurate to get information about spatial variability of the snow melt timing and rates, especially at the areas where available snow measurements are not representing the area under interest and previously unexplored regions. With wireless connections the method could also be used for obtaining real rime data of the snow melt.

8 REFERENCES

AHC 2015. Alpine Hydro Climatology research team of the Institute of Geography at the University of Innsbruck [internet]. Available: http://www.alpinehydroclimatology.net/ [referred 28.4.2015].

Barnett, T.P., Adam, J.C. & Lettenmaier, D.P. 2005. "Potential impacts of a warming climate on water availability in snow-dominated regions". Nature, vol. 438, no. 7066, pp. 303-309.

Bras, R.L. 1990. Hydrology: an introduction to hydrologic science. Reading, MA: Addison-Wesley, 642 p. ISBN 0-201-05922-3

Campell Scientific 2011. Instruction manual. SR50A Sonic Ranging Sensor [internet]. Available: http://s.campbellsci.com/documents/us/manuals/sr50a.pdf [publication date unknown, referred 28.4.2015].

CNRM-GAME 2015. French National Centre for Meteorological Research - Research group of atmospheric meteorology. Snowpack models [internet]. Available: http://www.cnrm-game.fr/spip.php?rubrique73&lang=en [referred 28.4.2015].

DeWalle, D. R., Henderson, Z., & Rango, A. (2002). Spatial and temporal variations in snowmelt degree-day factors computed from SNOTEL data in the Upper Rio Grande basin. In Proceedings of the Western Snow Conference (Vol. 70, p. 73). Colorado State University.

DeWalle, D.R. and Rango, A. 2011. Principles of Snow Hydrology. Cambridge University Press, 410 p. ISBN 978-0-521-29032-6

Dingman, S.L. 2008. Physical hydrology, 2nd edition. Upper Saddle River, NJ: Prentice Hall, 646 p. ISBN 1-57766-561-9

Drebs A., Nordlund A., Karlsson P., Helminen J., Rissanen P. 2002. Tilastoja Suomen ilmastosta 1971 - 2000 - Climatological Statistics of Finland 1971 - 2000. Ilmastotilastoja Suomesta 2002:1, Ilmatieteen laitos, Helsinki, 100 p.

FMI 2015. Finnish Meteorological Institute – Snow statistics [internet]. Available: http://en.ilmatieteenlaitos.fi/snow-statistics [referred 11.5.2015].

Førland E.J. (ed.), Allerup P., Dahlström B., Elomaa E., Jónsson T., Madsen H., Perälä J., Rissanen P., Vedin H. & Vejen F. 1996. Manual for operational correction of Nordic precipitation data. Oslo, Norwegian Meteorological Institute. 66 p. ISSN 0805-9918

GIMP 2015. GNU Image Manipulation Program [internet]. Available: http://www.gimp.org/ [referred 11.5.2015].

Gray, D.M. and Male D.H. 1981. Handbook of snow: Principles, processes, management & use. Toronto: Pergamon Press, 776 p. ISBN 0080253741

Hock, R. 2003. Temperature index melt modelling in mountain areas. Journal of Hydrology, vol. 282, no. 1, pp. 104-115.

IPCC 2013a: Annex III: Glossary [Planton, S. (ed.)]. In: Climate Change 2013: The Physical Science Basis. Contribution of Working Group I to the Fifth Assessment Report of the Intergovernmental Panel on Climate Change [Stocker, T.F., D. Qin, G.-K. Plattner, M. Tignor, S.K. Allen, J. Boschung, A. Nauels, Y. Xia, V. Bex and P.M. Midgley (eds.)]. Cambridge University Press, Cambridge, United Kingdom and New York, NY, USA.

IPCC 2013b: Summary for Policymakers. In: Climate Change 2013: The Physical Science Basis. Contribution of Working Group I to the Fifth Assessment Report of the Intergovernmental Panel on Climate Change [Stocker, T.F., D. Qin, G.-K. Plattner, M. Tignor, S.K. Allen, J. Boschung, A. Nauels, Y. Xia, V. Bex and P.M. Midgley (eds.)]. Cambridge University Press, Cambridge, United Kingdom and New York, NY, USA.

Jonckheere, I., Nackaerts, K., Muys, B., & Coppin, P. 2005. Assessment of automatic gap fraction estimation of forests from digital hemispherical photography. Agricultural and Forest Meteorology, 132(1), 96-114.

Jones, H.G. 2001. Snow ecology: an interdisciplinary examination of snow-covered ecosystems. Cambridge University Press, 400 p. ISBN 978-0-521-58483-8

Jordan, R. (1991). A one-dimensional temperature model for a snow cover, technical documentation for SNTHERM.89. In Cold Regions Research and Engineering Laboratory Special report 91-16. Hanover, NH: US Army, Corps of Engineers.

Korhonen, L., & Heikkinen, J. 2009. Automated analysis of in situ canopy images for the estimation of forest canopy cover. Forest Science, 55(4), 323-334.

Kuusisto, E. 1984. Snow accumulation and snowmelt in Finland. Helsinki, National Board of Waters: Publications of the Water Research Institute 55, 149 p. ISBN 951-46-7494-4

Kuusisto E. & 1986. Järvet ja Itämeri. In Mustonen S. (Edt.) Sovellettu hydrologia. Helsinki, Vesiyhdistys r.y, p. 256-290. ISBN 951-95555-1-X

Liwata, P., Hänninen, P., Okkonen, J. & Sutinen, R. 2014. Time-stability of soil water through boreal (60–68° N) gradient. Journal of Hydrology, vol. 519, pp. 1584-1593.

Lundquist, J. D., & Lott, F. 2008. Using inexpensive temperature sensors to monitor the duration and heterogeneity of snow-covered areas. Water Resources Research, 44(4).

Marks, D., Dozier, J., & Davis, R. E. (1992). Climate and energy exchange at the snow surface in the alpine region of the Sierra Nevada: 1. Meteorological measurements and monitoring. Water Resources Research, 28(11), 3029-3042.

Meløysund, V., Leira, B., Høiseth, K.V. & Lisø, K.R. 2007. Predicting snow density using meteorological data. Meteorological Applications, vol. 14, no. 4, pp. 413-423.

NASA 2012. Global Precipitation Measurement Mission Brochure [internet]. Available: http://www.nasa.gov/sites/default/files/files/GPM_Mission_Brochure.pdf [publication data unknown, referred 28.4.2015].

Okkonen, J. & Kløve, B. 2011. A sequential modelling approach to assess groundwater–surface water resources in a snow dominated region of Finland. Journal of Hydrology, vol. 411, no. 1, pp. 91-107.

Onset 2015. HOBO® Pendant® Temperature Data Logger (UA-001-xx) Manual [internet]. Available: http://www.onsetcomp.com/files/manual_pdfs/9531-K-MAN-UA-001.pdf [Publication date unknown, referred 16.3.2015].

Peel, M.C., Finlayson, B.L. & McMahon, T.A. 2007. Updated world map of the Köppen-Geiger climate classification. Hydrology and earth system sciences discussions, vol. 4, no. 2, pp. 439-473.

Pirinen, P., Simola, H., Aalto, J., Kaukoranta, J., Karlsson, P. & Ruuhela, R. 2014. Climatological statistics of Finland 1981 – 2010. Helsinki: Finnish Meteorological Institute, 83 p. ISBN 978-951-697-766-2

Pomeroy, J. and Brun, E. 2001. Physical properties of snow. In Jones, H., Pomeroy, J., Walker, D. and Hoham, R. (Edt.) Snow ecology: an interdisciplinary examination of snow-covered ecosystems. Cambridge University Press. 201. USA.

R Core Team 2014. R: A language and environment for statistical computing. R foundation for Statistical Computing, Vienna, Austria. Available: http://www.R-project.org/

R-Manual 2015. Test for Association/Correlation between Paired Samples. The R-manuals [internet]. Available: https://stat.ethz.ch/R-manual/R-devel/library/stats/html/cor.test.html [publication data unknown, referred 21.5.2015].

Rasmus, S. 2005. Snow Pack Structure Characteristics in Finland: Measurements and Modelling, Helsinki, University of Helsinki: Report Series in Geophysics No.48, 238 p. ISBN 952-10-2379-1

Reusser, D. E., & Zehe, E. 2011. Low-cost monitoring of snow height and thermal properties with inexpensive temperature sensors. Hydrological Processes, 25(12), 1841-1852.

SLF 2015. Swiss Federal Institute for Snow and Avalanche Research. Modeling [internet]. Available: http://www.slf.ch/forschung_entwicklung/modellieren/index_EN [referred 28.4.2015].

Sutinen, R., Äikää, O., Piekkari, M. & Hänninen, P. 2009. Snowmelt infiltration through partially frozen soil in Finnish Lapland. Geophysica, vol. 45, no. 1-2, pp. 27-39.

Sutinen, R., Närhi, P., Middleton, M., Hänninen, P., Timonen, M. & Sutinen, M. 2012. Advance of Norway spruce (Picea abies) onto mafic Lommoltunturi fell in Finnish Lapland during the last 200 years. Boreas, vol. 41, no. 3, pp. 367-378.

SYKE 2014. Finnish Environment Institute. Remote Sensing products – Fractional Snow Cover in Baltic Sea Region [internet]. Available: http://wwwi4.ymparisto.fi/i4/eng/snow/fsc_baltic_eng.html [publication data unknown, referred 27.4.2015].

USACE 1956. Snow Hydrology, Summary Report of the Snow Investigations. Portland, OR: N. Pacific Div., COE.

USGS 2015. U.S. Geological Survey – The Water Cycle [internet]. Available: http://water.usgs.gov/edu/watercycle.html [Publication data unknown, referred 27.4.2015].

Vajda, A., Venäläinen, A., Hänninen, P. & Sutinen, R. 2006. Effect of vegetation on snow cover at the northern timberline: a case study in Finnish Lapland. Silva Fennica, vol. 40, no. 2, pp. 195.

Vehviläinen, B. 1992. Snow cover models in operational watershed forecasting. Helsinki, National Board of Waters and the Environment: Publications of water and environmental research institute, 112 p. ISBN 951-47-5712-2

Veijalainen, N., Jakkila, J., Nurmi, T., Vehviläinen, B., Marttunen, M. & Aaltonen, J. 2012. Finland's water resources and climate change – Effects and adaptation, final report of the WaterAdapt – project. Helsinki, Finnish Environment Institute: The Finnish Environment 16/2013, 138 p. ISBN 978-952-11-4018-1

Annex 1. Field measurement results on 16 - 17th of April 2014.

Site, ST	Snow Depth (m)	Mass (kg)	Mass snow (m)	SWE (mm)	Density (kg m^{-3})
2.1	0.73	3.05	1.70	204	280.0
2.2	0.75	3.17	1.82	219	291.7
2.3	0.73	3.10	1.75	210	288.2
2.4	0.91	3.48	2.13	256	281.3
2.5	0.83	3.39	2.04	245	295.4
3.1	0.79	3.03	1.68	202	255.7
3.2	0.91	3.56	2.21	266	291.9
3.3	0.99	3.83	2.48	298	301.0
3.4	0.92	3.64	2.29	275	299.1
3.5	0.94	3.73	2.38	286	304.3
4.1	0.73	2.97	1.62	195	266.8
4.2	0.81	3.54	2.19	263	324.9
4.3	1.11	3.136	3.14	376	339.1
4.4	0.65	2.87	1.52	183	281.2
4.5	0.83	3.54	2.19	263	317.1
5.1	0.82	3.53	2.18	262	319.5
5.2	0.86	3.59	2.24	269	313.0
5.3	1.16	3.26	3.26	391	336.9
5.4	0.83	3.79	2.44	293	353.2
5.5	0.79	3.25	1.90	228	289.1
6.1	0.79	3.03	1.68	202	255.7
6.2	0.94	4.04	2.69	323	343.8
6.3	0.78	3.32	1.97	237	303.6
6.4	0.79	2.71	1.36	164	207.1
6.5	0.75	3.16	1.81	218	290.1
7.1	0.88	2.90	1.55	186	211.8
7.2	0.98	3.46	2.11	254	258.8
7.3	0.87	3.60	2.25	270	310.8
7.4	0.88	3.62	2.27	273	310.0
7.5	0.84	3.19	1.84	221	263.3

Annex 2. Model results for overall and plot specific DDF.

Difference between modelled and measured day for complete snow melt in days. Median of all determined DDF's used. Overall mean and median: 0.04 & 0. SD 3.89, IQR 5. RMSE = 3.81.

	ST2	**ST3**	**ST4**	**ST5**	**ST6**	**ST7**
1	-3	-1	0	3	-4	-11
2	1	NA	4	4	3	-5
3	-3	0	6	6	1	-2
4	-1	5	-1	3	-6	-1
5	0	NA	4	2	-2	1
Mean / SD	-1.2 / 1.79	1.33 / 3.21	2.6 / 2.97	3.6 / 1.52	-1.6 / 3.65	-4 / 4.24
Median / IQR	-1 / 3	0 / 3	4 / 4	3 / 1	-2 / 5	-2 / 4

Difference between modelled and measured day for complete snow melt in days. Median DDF of each experiment plot. Overall mean and median: -0.46 & -1. Overall SD and IQR: 3.21 & 4.25. RMSE = 3.19.

	ST2	**ST3**	**ST4**	**ST5**	**ST6**	**ST7**
1	-5	-1	-1	-1	-3	-6
2	-1	NA	2	0	4	-2
3	-6	0	4	3	2	1
4	-5	5	-2	2	-5	2
5	-3	NA	2	-1	-2	4
Mean / SD	-4 / 2	1.33 / 3.21	1 / 2.45	0.6 / 1.82	-0.8 / 3.7	-0.2 / 3.9
Median / IQR	-5 / 2	0 / 3	2 / 3	0 / 3	-2 / 5	1 / 4